Developing the Techniques for Raman, Surface-Enhanced Raman Scattering (SERS), and Fluorescence Spectroscopies of Organic Molecules in Isolation

By

Jonathan Wolfe

A thesis submitted to the faculty of the University of Mississippi in partial fulfillment of the requirements of the Sally McDonnell Barksdale Honors College

Oxford

May 2010

Approved by

_____
Advisor: Professor Nathan Hammer

_____
Reader: Professor Gregory Tschumper

_____
Reader: Professor Randy Wadkins

1 Fundamentals of Spectroscopy

The nature of matter and light has been a subject of philosophical debate since antiquity. However, by the end of the nineteenth century, much of the scientific community believed that most of the significant principles that govern the natural world had been discovered. Classical physics was able to explain complex phenomena such as planetary motions, elasticity, and hydrodynamics. The field of thermodynamics had been developed nearly to completion by James Joule, Sadi Carnot, Josiah Gibbs, et al. The magnetic and electronic nature of light had been demonstrated by James Clerk Maxwell's famous equations. In the neighboring field of chemistry, a periodic table had been developed with a self-consistent set of atomic masses assigned to each element. The fundamental principles of chemical reactions had been elucidated by Svante Arrhenius. Due to these and other incredible strides in physics and chemistry, many scientists believed that the future of the physical sciences would consist of measuring constants to more decimal places, and classifying an endless number of chemical reactions. Only a few confounding problems existed, including an explanation of blackbody radiation that was consistent with experiment. The explanation provided by Max Planck and later corroborated by Albert Einstein started the quantum upheaval that forever changed the picture of the subatomic world. Decades of applied quantum mechanics have culminated in the science of spectroscopy. This senior honors thesis deals with the development of several spectroscopic techniques and their applications in analyzing chemical systems.

1.1 Transitions Between Energy Levels

Spectroscopy can be defined as the study of the interaction between matter and light, or alternatively as applied quantum mechanics. Spectroscopy is able to experimentally verify the discrete energy levels mathematically calculated using quantum mechanical models. By investigating these energy levels, a vast array of chemical and physical information can be extracted from the system being studied.

One of the most fundamental concepts involved in spectroscopy is energy. Energy is not readily defined in terms of observable quantities. Instead, energy is intrinsically related to movement. Each of the energy levels that spectroscopy deals with corresponds to specific movements in a molecular or atomic system. Consequently, an explanation of spectroscopy must necessarily start with a description of these movements.

A molecule can be considered a stable system of electrons and nuclei. A molecular system with M nuclei and N electrons has 3(M+N) degrees of freedom. Degrees of freedom simply represent the three dimensions of space in which nuclei and electrons can move. For a given molecule, the nuclei can be fixed in space according to the Born-Oppenheimer approximation[0]. The system can now be associated with a Lewis structure, and a molecular point group. 3N degrees of freedom describe the motion of electrons around the frozen frame. The energy of motion of the electrons is called electronic energy, $E_{electronic}$. If the molecule is regrouped into M atoms, the molecule now has 3M degrees of freedom. With the nuclei of the molecule still fixed in space relative to one another, a single point can be defined as the center of mass. Movement of this center of mass is associated with translation motion and can account for three degrees of freedom. Rotations around this center of mass can be described by three rotational

degrees of freedom (two for linear molecules). The remaining 3M-6 degrees of freedom (3M-5 for linear molecules) are due to molecular vibrations in which the nuclei move relative to one another. Each of these motions is paired with its associated energy. As a first approximation, the total energy of the system is now:

$$E = E_{electronic} + E_{vibrational} + E_{rotational} + E_{translational} \quad (1.1)$$

The magnitude of each of these types of energy can change depending on how the subunits of the molecule move. Additionally, each of these types of energy is quantized, meaning they can only occur at discrete values or levels. Molecules can undergo transitions between energy levels due to the addition or subtraction of energy. In traditional spectroscopy, such transitions are effected by light.

There are two different but complementary models that explain the nature of light. In one model, light is considered a transverse wave made up of electric and magnetic fields oscillating perpendicular to one another. Thus, light can be described as electromagnetic radiation. Descriptions of light waves are characterized by properties such as wavelength, frequency, amplitude, and speed of propagation. The wave model is able to account for physical properties of light such as superposition, refraction, reflection, and dispersion among others. However, there are some phenomena for which the alternate particulate model of light is better suited to explaining. In the particulate model, light is considered a stream of tiny packets of energy called photons. The energy of a photon is given by the equation:

$$E = h\nu \quad (1.2)$$

where E is energy, h is the Planck constant, and ν is the frequency of light. The particulate model of light can better account for the transfer of energy that occurs between light and matter in the case of transitions between energy levels.

At room temperature, most chemical species are in their *ground state*. The ground state is the lowest possible energy state of a molecule. Molecules can absorb energy in the form of light, which causes a permanent transfer of energy to the absorbing medium. When this happens, molecules are promoted to an *excited state*. In order for absorption to occur, the energy of the incident light given by equation (1.2) must exactly equal the difference in energy between the ground state and the excited state. An excited state can correspond to any of the types of energy levels given in equation (1.1). However, quantum postulates called selection rules dictate that only certain transitions are physically allowed. The magnitude of the difference between electronic, vibrational, rotational, and translational energy levels varies significantly. The difference between energy levels occurs in the order:

$$\Delta E_{Electronic} > \Delta E_{Vibrational} > \Delta E_{Rotational} > \Delta E_{Translational}$$

The difference between translational energy levels is too small to be resolved by modern spectroscopic techniques so they will not be considered. For most molecules, there exist many more vibrational energy levels than electronic energy levels. Additionally, there are more rotational energy levels than vibrational energy levels. Thus, between electronic energy levels there are several vibrational energy levels, and between vibrational energy levels there are several rotational energy levels. Figure 1.1 is a diagram showing electronic and vibrational energy levels for a diatomic and illustrating the absorption

process described above and the emission process described in the next paragraph. Rotational states have been omitted.

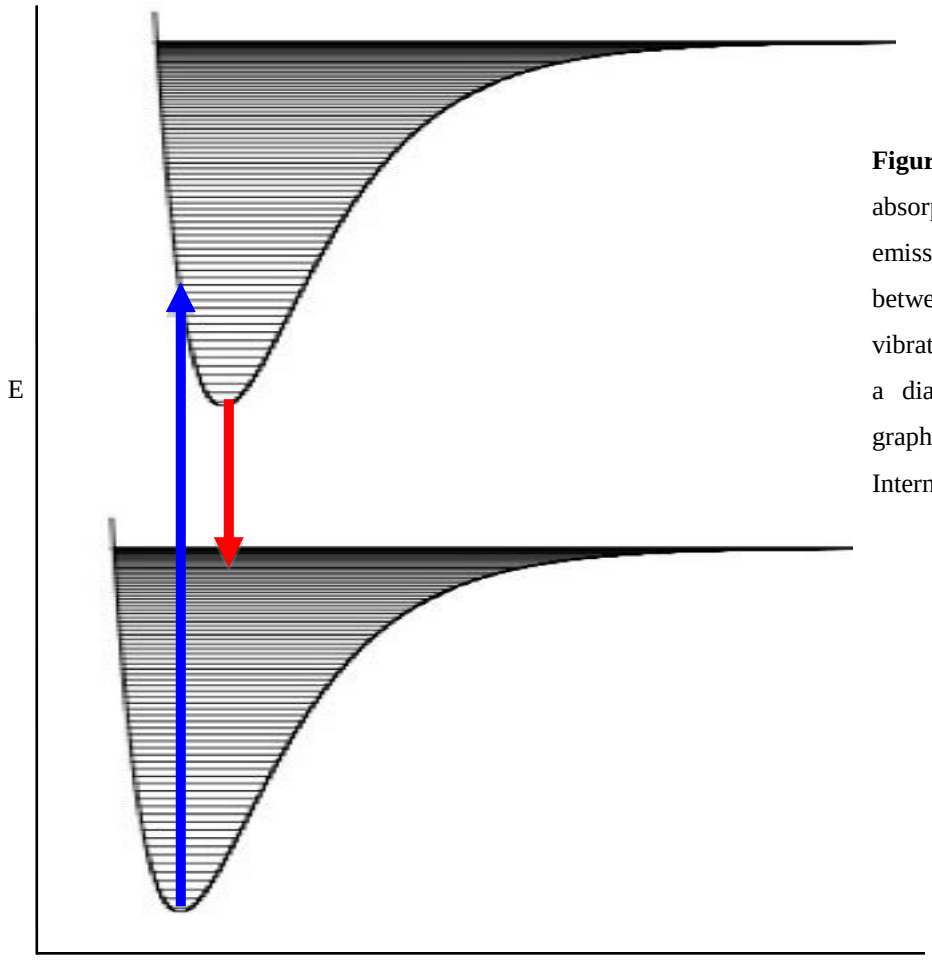

Figure 1.1 Shows the absorption (blue) and emission (red) processes between electronic and vibrational energy levels for a diatomic displayed on a graph of Energy (E) vs. Internuclear Distance.

The excited state lifetime of a molecule is generally brief. The lifetime is on the order of 10^{-8} seconds for an electronic excited state and 10^{-15} seconds for a vibrational excited state[8]. This is a result of the tendency in nature to restore energy populations to their equilibrium values. A molecule in an excited state can relax to a lower energy state by a radiative or nonradiative transition. In a nonradiative transition, the molecule relaxes into a lower energy state while the released energy is essentially dissipated as heat. In a

radiative transition, relaxation involves the emission of light isotropically as luminescence. The emission of light can be *stimulated* or *spontaneous* depending on the conditions in which it occurs. Stimulated emission requires a precise set of experimental conditions and will not be considered. The more common spontaneous emission can occur as *fluorescence* or *phosphorescence*, which is emission from an excited state with the same or different spin multiplicity relative to the ground state respectively. Interestingly, spontaneous emission can occur in the absence of stimulating photons. Other extremely important light-matter interactions are scattering and transmission. The scattering of light and its utilization in Raman spectroscopy is described in chapter 2.

1.2 Rotational, Vibrational, and Electronic Spectroscopies and Instrumentation

Different types of spectroscopy can be delineated by the type of energy level transitions they produce. Electronic, vibrational, and rotational spectroscopies necessitate distinctive theoretical and experimental considerations. A brief discussion of each follows.

As described previously, the rotational motion of molecules around a fixed center of mass gives rise to rotational energy levels. Quantum mechanical treatment of rotating molecules gives energy levels incrementally in terms of the rotational quantum number J. In rotational spectroscopy, the microwave and far-infrared regions of the electromagnetic spectrum are of appropriate energy to cause transitions between rotational energy levels. Knowledge of these transitions can elucidate geometrical structure, internuclear distances, and dipole moments in molecules. Unfortunately, rotational spectroscopy has severe limitations in that with few exceptions, the system under study must have a permanent dipole moment and must be in the gas phase. Without a permanent dipole

moment, an applied electric field in the form of light would not be able to cause sufficient torque for rotations. The gas phase requirement is due to the motional constraint of molecules closely packed in solution or within the crystal lattice of a solid.

In a molecule, the motions of individual atoms relative to one another give rise to vibrational energy levels. Vibrational energy levels are associated with the quantum number v. The two types of vibrations for a multiatomic system are stretches and bends. Stretching implies vibration along the line of a bond, which changes bond length. Bending changes bond angles. The 3M-6 degrees of freedom in a molecule correspond to independent *normal modes* of vibration. In each normal mode, every atom in the molecule vibrates with the same frequency and all atoms pass through their equilibrium positions simultaneously[4]. However, the amplitude of the vibrations of individual bonds can be radically different. The vibrational energy levels of molecules can be probed by infrared radiation or by Raman spectroscopy. Using these methods, the molecular structure of a molecule can be found. In order for infrared radiation to produce a vibrational transition, there must be a change in the dipole moment of the sample. Infrared radiation is also of sufficient energy to cause rotational transitions due to the numerous rotational energy levels between each vibrational energy level. Consequently, a vibrational spectrum can display rotational fine structure if the system under study is in the gas phase and has a permanent dipole moment.

Electronic spectroscopy involves transitions of electrons between various molecular orbitals. Because a given electronic state contains several vibrational and rotational states, electronic spectroscopy includes the previously discussed concepts concerning vibrational and rotational energy levels. Common regions of the

electromagnetic spectrum used in electronic spectroscopy are the visible and ultraviolet regions. Light from these regions has sufficient energy to cause electronic transitions in the valence electrons of a molecule. The higher energy x-ray region can cause transitions of core electrons. A gas phase electronic spectrum can exhibit vibrational and rotational fine structure. The density of these states becomes too difficult to resolve if the molecule under study is large, i.e. with a very high number of possible rotational and vibrational levels. The rovibrational fine structure of an electronic spectrum can also be blurred by solvent effects.

All previous discussions have been based on the light-matter interactions of molecules. Atomic spectroscopy is very different in that single atoms cannot vibrate or rotate, and thus have only electronic energy levels. Electronic absorption and emission processes are the same just without the convolutions of vibrational and rotational energy levels.

Energy levels must be displayed in such as way as to allow interpretation in order to extract the chemical and physical information desired. A spectrum is a plot that gives this information in relevant terms. Spectra are obtained through the use of various instruments. A block diagram illustrating the basic process of spectroscopic data collection is shown in figure 1.2.

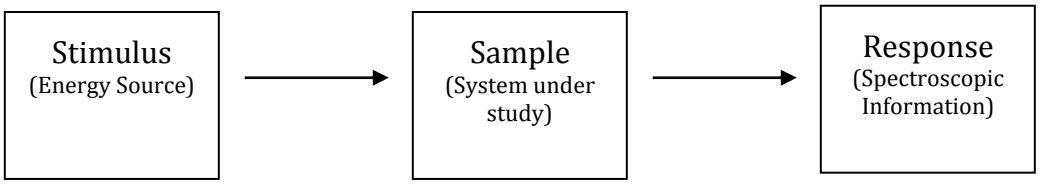

Figure 1.2 shows a block diagram illustrating the basic components involved in the collection of spectroscopic data.

The stimulus generally consists of a light source used to cause transitions between energy levels. The energy of the light used must be appropriate for the type of energy level transitions desired. Light sources can be either continuum sources, or line sources. Continuum sources produce light with variable intensity over a wide range of wavelengths. Other devices must be used in tandem with continuum sources to allow selection of narrow wavelength ranges. Continuum sources include gas-filled arc or deuterium lamps for the ultraviolet and visible regions, heated solids for the infrared region, or klystron tubing for the microwave region. Line sources emit light with an extremely narrow wavelength range. Lasers, and mercury and sodium lamps are examples of line sources. The sample is obviously the chemical system to be analyzed. Most spectroscopic analyses require devices that can allow selection for narrow wavelength regions of the electromagnetic spectrum. The two main types of wavelength selectors are filters and monochromators. Filters can select narrow wavelength ranges through the properties of interference or absorption. Monochromators disperse light into its component wavelengths through the use of diffraction gratings or prisms. The light collected after interaction with the sample is termed the response. This light is generally collected by a detector or a sensor. There are many types of detectors used in each type of spectroscopy. Generally, the detector acts as a signal transducer. A transducer converts physical or chemical information into an electronic data domain. The electronic data is then converted to a readout that is interpretable by the user.

1.3 References

(1) McHale, J. L. *Molecular Spectroscopy*; Prentice Hall: New Jersey, **1999**.

(2) Herzberg, G. *Molecular Spectra and Molecular Structure I. diatomic molecules*; Van Nostrand and Reinhold Company: New York, **1939**.

(3) Herzberg, G. *Molecular Spectra and Molecular Structure II. Infrared and Raman Spectra of Polyatomic Molecules*; Van Nostrand Reinhold Company: New York, **1945**.

(4) Colthup, N. B.; Daly, L. H.; Wiberley, S. E. *Introduction to Infrared and Raman Spectroscopy*; Academic Press, Inc.: New York, **1990**.

(5) Bruice, P. Y.; *Organic Chemistry*; Prentice Hall: New Jersey, **2007**.

(6) McQuarrie, D.; *Quantum Chemistry*; University Science Books: California, **2008**.

(7) Aroca, R.; *Surface-Enhanced Vibrational Spectroscopy*; John Wiley & Sons, ltd: England, **2006**.

(8) Skoog, D. A.; Holler, F. J.; Crouch, S. R.; *Principles of Instrumental Analysis*; Brooks/Cole: United States, **2007**.

2 Raman and Surface-Enhanced Raman Scattering Spectroscopy

When electromagnetic radiation interacts with matter, the energy can be absorbed, transmitted or scattered. The absorption process described in chapter one occurs when the energy of the incident radiation, given by the equation $E = h\nu$, exactly matches the difference between the ground state and a rotational, vibrational, or electronic excited state. Transmission of radiation refers to the passage of radiation through a transparent medium. The final possibility for light-matter interaction is isotropic reemission in the form of scattering. Raman and SERS spectroscopies utilize the process of inelastic light scattering to determine the energies of vibrational modes.

2.1 Light Scattering and the Raman Effect

The scattering process of radiation has been investigated since the nineteenth century. A classical approach to light scattering can be described as follows: assuming no absorption, when light falls on a substance it induces a temporary polarization, or separation of charge, between the nuclei and electrons that make up the substance. The induced polarization can be represented as a simple dipole. The magnitude of the induced dipole moment is dependent on the electric field component of electromagnetic radiation as given by equation (2.1).

$$\mu = \alpha E \qquad (2.1)$$

where μ represents the dipole moment, E is the strength of the electric field, and α is a proportionality term called the polarizability of the bond. The polarizability describes the extent to which the electron cloud is deformed during polarization. The value of the polarizability may not be constant due to variation from molecular vibrations and rotations. The electric field strength of electromagnetic radiation varies with time according to the equation (2.2).

$$E = E_0 \cos 2\pi\nu t \tag{2.2}$$

where E_0 is the maximum strength of the electric field, ν is the frequency of the radiation, and t is time. Combining equations (2.1) and (2.2) provides an expression for an oscillating dipole moment.

$$\mu = \alpha E_0 \cos 2\pi\nu t \tag{2.3}$$

As shown in equation (2.2), the electric field strength of light oscillates sinusoidally. Consequently, the induced dipole shown in equation (2.3) also oscillates sinusoidally with the same frequency as the incident radiation. Moving charged particles create electric fields, which in turn create magnetic fields. The two fields combine to produce electromagnetic radiation of the exact same frequency as the incident radiation. Emission of this radiation follows. Destructive interference caused by the wave property of superposition partially prevents propagation of this newly reemitted radiation in any direction except that of the original light path. However, a small portion is emitted in all directions as scattered light. When the scattered light possesses the same frequency as the incident light, the scattering is termed *elastic*. This type of scattering is also called *Raleigh Scattering*, after Lord Raleigh, who showed in 1871 how the wavelength

dependence of light scattered by small particles in the atmosphere could account for the blue color of the sky.

When the frequency and thus the energy of scattered light is different from that of the incident light, the scattering is termed *inelastic*. This phenomenon was first discovered in 1922 by Arthur Holly Compton in his studies of the x-ray region of the electromagnetic spectrum. The Compton effect refers to the shift of scattered monochromatic x-rays to lower frequency after interaction with matter to eject an electron. The following year Adolf Smekal derived a mathematical expression predicting inelastic light scattering. Similar derivations were repeated between 1923 and 1927 by Kramers and Heisenberg, Schrodinger, and Dirac. Despite the predictions, the theory needed experimental validation due to an inability of mathematics to completely describe the scattering phenomenon. In 1922, an Indian physicist named C. V. Raman began this experimental work that led to his eponymous effect while trying to find the optical analog to the Compton scattering of x-rays.

It took C.V. Raman six years before producing publishable data on his effect. This was partially due to the tiny probability of inelastic scattering when compared with elastic scattering. Only 1 in approximately every 10^8 photons experiences the characteristic frequency change. Additionally, the instrumentation used to obtain these first spectra was humble at best. Sunlight was focused through a telescope in tandem with a focusing lens. Colored filters were used to select the various wavelengths of interest. The focused light fell on a purified sample liquid or vapor, and the spectrum was projected onto photographic plates. Exposure times using this method could be as long as 180 hours. Despite the difficulties, Raman was able to use this method and others to

obtain spectra of over 60 liquids and vapors. He was able to distinguish the inelastically scattered light from fluorescence due to its strong polarization. His articles on the subject first appeared in the Indian Journal of Physics and subsequently the journal Nature. He noticed, as did others that the energy differences between the incident light and inelastically scattered light were exactly equal to the spacing between the vibrational energy levels of the molecules under study. His work earned him the 1930 Nobel Prize in physics and opened to the world a new method to investigate vibrational energy levels.

In a Raman spectrometer, monochromatic light illuminates a sample in its energetic ground state or an excited vibrational state. The frequency of the light is generally such that it has too much energy to cause a single vibrational transition, but too little energy to cause an electronic transition. A portion of this light is then scattered. This process can first be described as promotion of a molecule to a virtual energy level. Virtual energy levels are not quantized, and thus the frequency of the excitatory radiation is not important as long as it does not promote absorption. Virtual energy levels are inherently unstable, and have an infinitesimally small lifetime. In the case of Rayleigh scattering, a molecule is excited from the ground state to a virtual energy level, followed by immediate relaxation back to the ground state. For inelastic scattering, there are two different possibilities. If the molecule is excited from a ground state to a virtual energy level, it can relax back to a vibrational excited state. This produces light lower in frequency, and thus energy, than the incident light by an amount equal to the difference between the ground state and the vibrational excited state. The shift of the scattered light to a lower frequency is called a *Stokes Shift*, a term borrowed from fluorescence spectroscopy. If the molecule is promoted from an excited vibrational state to a virtual

state, scattered radiation produced by relaxation to the ground state will possess a frequency and energy greater than that of the incident radiation. This shift to a greater frequency is called an *Anti-Stokes Shift*. Molecules at ambient temperature are generally in their energetic ground state, so the intensity of the Stokes scattered light is far greater than its Anti-Stokes counterpart. As mentioned in chapter one, infrared radiation, i.e. heat, is of the appropriate energy to cause vibrational energy level transitions. Consequently, for a given vibration, the ratio of the number of species in an excited vibrational state to the ground state depends strongly on temperature as given by equation (2.4).

$$N_1/N_0 = e^{-(h\,\nu_m/k_b\,T)} \qquad (2.4)$$

where N_1 and N_0 represent the number of species in the first excited vibrational state and the ground state respectively, h is the plank constant, ν_m is the frequency of the vibration, k_b is the Boltzmann constant, and T is temperature. Because the relative population ratio provided by equation (2.4) strongly favors the ground state at room temperature, a Raman Spectrum generally consists of only the Stokes shifted peaks. Figure 2.1 shows diagram illustrating the Rayleigh, Stokes, and Anti-Stokes scattering processes.

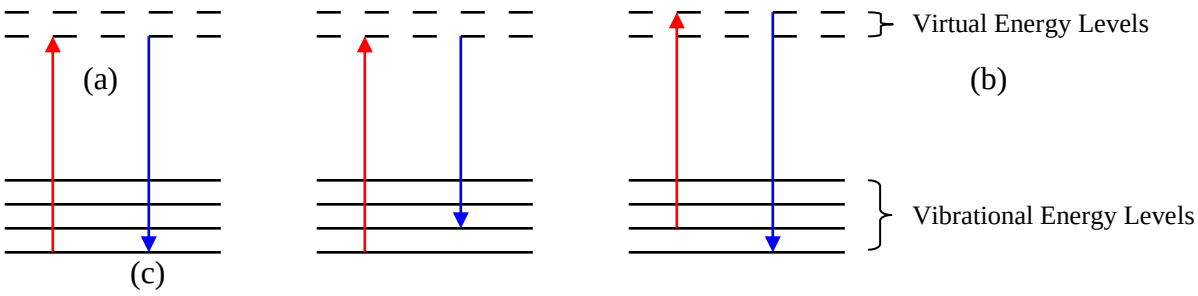

Figure 2.1 displays energy level diagrams illustrating **a)** Rayleigh Scattering **b)** Stokes Raman Scattering **c)** Anti-Stokes Raman Scattering

The classical description of light scattering including the oscillating dipole moment given in equation (2.3) can be expanded to include Raman Scattering. As mentioned previously, the polarizability of a bond may not have a constant value. As the bond length changes due to molecular vibrations, light will interact differently with the electron cloud at different displacements from the equilibrium value. As subsequently derived, it is this change in polarizability that gives rise to the Raman activity of molecules. For a homonuclear diatomic, molecular vibrations can be modeled as two masses connected by a spring that oscillates harmonically. Using this model, the polarizability for small displacements can be expanded in a Taylor series.

$$\alpha = \alpha_0 + (\partial\alpha/\partial Q)\, Q + \ldots \tag{2.5}$$

where α_0 is the polarizability at the equilibrium bond length, and Q is a normal coordinate which simply represents atomic displacements during normal modes of vibration. Assuming harmonic oscillation will allow higher order terms other than those given in equation (2.5) to be neglected. The normal coordinate Q varies periodically with the frequency of the normal mode ν_v according to the equation:

$$Q = Q_0 \cos(2\pi\nu_v t) \tag{2.6}$$

where Q_0 is the normal coordinate at the equilibrium position. Combining the two equations gives a new expression for the polarizability.

$$\alpha = \alpha_0 + (\partial\alpha/\partial Q)\, Q_0 \cos(2\pi\nu_v t) \tag{2.7}$$

Substituting the expression for α obtained in equation (2.7) into equation (2.3) gives the induced dipole moment in the form:

$$\mu = \alpha_0 E_0 \cos 2\pi\nu t + (\partial\alpha/\partial Q)\, Q_0 (\cos 2\pi\nu_v t)\, E_0 (\cos 2\pi\nu t) \tag{2.8}$$

the trigonometric identity [cos a cos b] = ½ [cos (a + b) + cos (a – b)] can then be used to convert equation (2.8) into:

$$\mu = \alpha_0 E_0 \cos 2\pi\nu t + (\partial\alpha/\partial Q)\, ½\, Q_0 E_0 [\cos 2\pi(\nu - \nu_v)t + \cos 2\pi(\nu + \nu_v)t] \qquad (2.9)$$

This equation gives the dipole moment in terms of three component frequencies, ν, $\nu - \nu_v$, and $\nu + \nu_v$. These frequencies correspond the Rayleigh, Stokes, and Anti-Stokes scattering respectively. Also, the intensity of the Raman scattered light is proportional to the square of the induced dipole μ. If the expression $(\partial\alpha/\partial Q)$ is zero, the radiating dipole only oscillates with the frequency of the incident radiation, and thus no Raman effect is observed.

Interpretation of Raman spectra can be based on the following considerations. As mentioned in chapter one, a molecule has 3N-6 vibrational degrees of freedom (3N-5 for linear molecules). These degrees of freedom describe normal modes of vibration, which coincide with vibrational energy levels. Vibrational energy level transitions give rise to peaks in a Raman Spectrum. The allowed vibrational energy level transitions are dictated by selection rules. Because different molecules have a unique set of normal modes, the Raman spectrum of each molecule is distinct. Some molecular vibrations occur with the same energy. These movements are said to be degenerate, and they are indistinguishable from each other in a Raman Spectrum. The relative energy of normal modes of vibration can often be determined based on the symmetry of the molecule. Applications of group theory can be used to correlate peaks in a Raman spectrum with specific normal modes.

The low intensity of Raman scattered light leads to experimental complications. The setup employed by C.V. Raman in the 1920s was not conducive to efficient data collection.

The necessity for intense sources of light to cause sufficient scattering made obtaining Raman spectra with sunlight or older lamps difficult. The photographic plates on which the original spectra were recorded needed long exposure times. The advent of lasers in the 1960s popularized Raman spectroscopy by providing the powerful, monochromatic light sources necessary for efficient data collection. At the same time, photographic plates were replaced by photomultiplier tubes: radiation transducers that can convert the energy of a single photon into an electrical signal. The later introduction of photo diode arrays and charge-coupled devices further contributed to the advancement of Raman spectroscopy by allowing instantaneous data collection of entire spectra with a sensitivity that rivaled that of the photomultiplier tube. Because of these and other technological progressions, Raman spectroscopy has become a useful tool for obtaining the structure and properties of molecules from their vibrational transitions.

2.2 Surface-Enhanced Raman Scattering (SERS) Spectroscopies

Obtaining vibrational energy levels from conventional Raman spectroscopy is often difficult due to the weak intensity of Raman Scattered light and because of the appearance of fluorescence. Surface-Enhanced Raman Scattering (SERS) Spectroscopy can be used to overcome these disadvantages. When molecules are adsorbed to specially roughed coinage metals, the metal nanostructure can combine with the incident light to produce a Raman signal enhancement greater than 10^{14}.

In 1974, M. Fleischmann et. al. published a paper concerning Raman studies of pyridine adsorbed to electrochemically roughened silver electrodes. The Raman spectra obtained in these studies showed enormous increases in intensity, which they attributed to the greater surface area provided by the electrode. In 1977, the research groups of

Albrecht and Creighton and Jeanmaire and Van Duyne independently concluded that an increase in surface area was not sufficient to explain the intense Raman signals obtained by Fleischmann et al. They suggested the enhancement of approximately 10^5 was due to a complex surface phenomenon involving interactions with surface plasmons in the silver electrode. The origin of the enhancement factor soon became hotly debated as numerous groups attempted to work out its specific mechanism. In this way, Surface-Enhanced Raman Spectroscopy found its way to the forefront of condensed matter physics and chemical physics communities.

SERS became a rapidly developing field as spectra of several different samples were taken. Additionally, it was shown that a large variety of metals besides silver could produce the characteristic enhancement. Initial SERS studies suggested that the enhancement of the Raman signal could be considered the product of two main contributions: an electromagnetic enhancement mechanism and a charge transfer mechanism. The electromagnetic mechanism was thought to be primarily responsible for the increased intensity, with the charge transfer mechanism providing secondary enhancement. This remains the general consensus, however some uncertainty still exists because separation of the two effects is virtually impossible.

The structure of the metallic substrate is of extreme importance to the SERS. The metallic substrate must be able to support radiative plasmon activity. Plasmons can be defined as the quanta of the oscillations of surface charges due to the interaction of a material with light. Furthermore, special roughening is required in order for surface plasmons to produce the characteristic enhancement. A more intuitive description of

plasmons and the SERS enhancement mechanisms using molecular orbital theory and band theory follows.

Molecular orbital theory is an excellent method to describe bonding in molecules. A fundamental premise of this theory is that the location of electrons in an atom can be modeled as probability distributions called orbitals. Atomic orbitals can be combined together to form bonding and antibonding molecular orbitals if the interaction is energetically favorable. For a homogeneous solid, such as a metallic substrate used in SERS, the atomic orbitals of a huge number of atoms combined in a linear fashion will produce molecular orbitals with very closely spaced energies. Low energy molecular orbitals with closely spaced energies can be combined to produce a low energy *band*. This band contains the electrons from the atoms and is called the *valence band*. Combinations of closely spaced atomic orbitals of higher energy form what is called a *conduction band*. The difference in energy between the valence band and the conduction band is called the *band gap*. In elements with filled valence bands, promotion of electrons to the conduction band is necessary for electrons to flow freely. If the material is an insulator, a large band gap can prevent this promotion causing electron movement to be restricted. If an element has only a partially filled valence band, the distinction between the valence band and the conduction band is blurred, and very little energy is needed to move electrons to higher energy levels within the band. Thus, these electrons are able to freely move throughout the solid. When an electron is promoted from the valence band to the conduction band, it leaves behind a hole. The free movement of electrons and holes is characteristic of a conductor. Figure 2.2 illustrates the band structure of an insulator and a conductor.

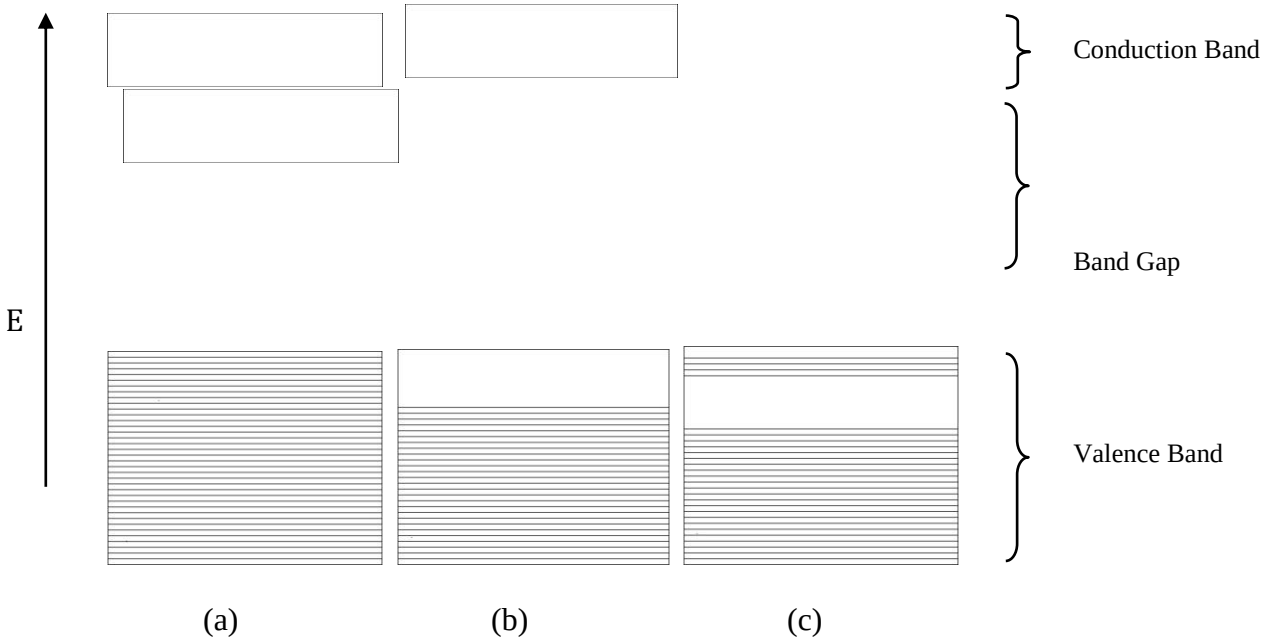

Figure 2.2 illustrates the band structure for insulators and conductors. **a)** insulator **b)** conductor with no stimulating energy applied **c)** conductor with stimulating energy applied causing free motion of electrons

Electromagnetic radiation of sufficient energy is able to promote electrons into a conduction band. In a many electron system, the simultaneous creation of electron-hole pairs is called excitons. The free electrons promoted to the conduction band are responsive to light. The electric field component of light can induce collective coherent oscillations in these electrons producing what is known as *plasmons*. These oscillating waves of conducting electrons are able to produce strong local electric fields. If the metallic surface is smooth, the electrons are only able to oscillate in a direction parallel to the surface, and the resulting electric field enhancement is contained within the metal. If the metal is specially roughened, the electric field is no longer confined and can radiate both parallel and perpendicular to the surface.

When considering the origin of the SERS enhancement it is helpful to recall that the Raman intensity is proportional to the square of the induced dipole. From equation (2.1) the induced dipole was shown to be equal to the product of the polarizability of the bond, α, and the strength of the electric field of the causative radiation, E. The metallic surface thus must influence one of these two factors. The electromagnetic enhancement can be seen to influence the strength of the electric field, and the charge transfer mechanism can be seen to alter the polarizability.

The electromagnetic enhancement mechanism stems from the excitation of surface plasmons. When a molecule adsorbed on a metal that supports plasmon activity is subjected to light, the local electric fields produced by surface plasmons can interact with the adsorbate to cause an increase in the intensity of scattered light. If the resulting radiation remains at or near resonance with the surface plasmons, the scattered radiation will again be enhanced. Thus, production of the most intense surface-enhanced Raman scattering is really due to frequency-shifted elastic scattering by the metal[0]. The electromagnetic enhancement is a long-range effect that can be detected over several layers of the adsorbate. It is worth noting that the electromagnetic enhancement is totally independent of the presence of an adsorbed molecule.

The charge transfer or chemical enhancement is due to the change in the symmetry properties of the molecule resulting from adsorption to the metal surface. Adsorption can be of two different types: physical adsorption (physisorption) or chemical adsorption (chemisorption). Physisorbed molecules adhere to surfaces through weak Van der Waals forces, and they are easily displaced. There is no significant redistribution of electron density in either the substrate or the adsorbate. Chemisorption involves a

chemical bond, i.e. a substantial rearrangement of electron density between the substrate and the adsorbate. This bond can be of completely ionic or covalent character or anywhere in between. The molecular orbitals of a chemisorbed molecule can interact with the conduction band of the metal. Electrons can then be easily transferred from the metal to the adsorbate and vice versa. Only molecules directly associated with the metal surface experience this enhancement, limiting this effect to the first monolayer of coverage. The SERS spectra of chemisorbed molecules can be unrecognizable from that of their Raman spectra due to the creation of the new chemical complex. Alternately, physisorbed molecules generally retain their identity and corresponding SERS spectra show no appreciable difference. The electronic and structural properties of the analyte involved are of great importance to the charge transfer enhancement, as opposed to the indiscretion of the electrochemical enhancement. The inability to separate the two effects has made a complete understand of the charge transfer enhancement mechanism elusive.

Careful control of the composition of the metal substrate is crucial to creating reliable SERS spectra. The roughening of metal surfaces is done to create nanoparticles smaller than the wavelength of the incident light. The resonant enhancement frequency of a metal substrate is a function of its dielectric constant, and the size and shape of the surface protrusions. Modulation of these factors can produce substrates that enhance radiation throughout the electromagnetic spectrum. A given substrate may provide proficient enhancement in one region, but poor enhancement in another. Therefore, a holistic approach is required when attempting to create the optimal substrate for a set of experimental conditions. SERS spectra have been observed from molecules adsorbed to silver, gold, copper, aluminum, lithium, and sodium, iron, and several other metals,

although silver and gold seem to give the best enhancement. Because substrate variability can so significantly affect the observed spectrum, substrate reproducibility is key to producing consistent results.

There are a wide variety of methods used to produce SERS substrates and each has its own advantages and disadvantages. The original SERS data was taken on silver electrodes that underwent several oxidation-reduction cycles. During these cycles, the metal of the electrode is first oxidized to a soluble compound. Subsequent reduction causes re-deposition of these species randomly over the metal surface, forming nanostructures. The enhancement achieved by this method can be as high as 10^6, and substrates show good stability. A major drawback to this method is the random and nonuniform distribution of particles, which leads to poor reproducibility. Vapor deposition of metals directly onto dielectric materials is a method to produce SERS substrates of similar quality to those obtained by electrochemical oxidation-reduction cycles. By controlling the temperature of the substrate and the deposition rate of the metal, films with different SERS activity can be produced. If the metal vapor is deposited onto a cold substrate (lower than 120 K), rough films are produced. Warmer temperatures increase the mobility of metal atoms, causing an aggregation of the metal nuclei to form "islands". Colloid solutions are an inexpensive way to produce SERS active substrates. A metal salt in an aqueous or nonaqueous solution is reduced by one of a variety of reductants. The liberated metal forms aggregates with the appropriate topography to provide extremely large enhancements. These colloids generally exhibit the greatest enhancement when they have a diameter between 50 nm and 100nm. The size, size distribution, and shape of the metal particles can be carefully controlled by varying

factors such as pH, temperature, and type of metal salt, or reductant. Stabilization of the colloids is accomplished by the addition of anions, which adsorb to the metal surface and prevent coagulation. Specially made colloids forming aggregates of two or more nanoparticles have been responsible for the enhancements as high as 10^{14}. Because of the available level of quality control, high reproducibility, and inexpensive cost, colloids solutions have become extremely popular.

SERS substrates with highly ordered, well-defined surfaces can be produced by chemical assembly and lithography techniques. Chemical assembly methods involve using coordinating molecules that can simultaneously bind analyte and metal to form an ordered structure. The coordinating molecule must be carefully selected depending on the properties of the analyte and the metal. Lithography techniques provide the greatest control in creating highly ordered substrates, and there are many available methods. One method is assembling an ordered array of polystyrene or silica spheres of the desired size on to a clean substrate. A metal film of the desired thickness is then deposited on this template by vapor deposition or electrochemical deposition, forming a SERS substrate. Another method involves layering a light sensitive material on to a solid glass silicon or gold film. Ultraviolet light or an electron beam is then used to pattern the photoresist, which after exposure and development can be used as a mold on which SERS active metals are deposited. Although chemical assembly and lithographic techniques can produce very highly ordered substrates the success of these methods often depends of the experience of the experimentalist and how strictly the experimental conditions can be controlled.

The SERS spectra of a given molecule can be vastly different from its Raman spectra due to the effects of the metal nanostructure. This can be partially attributed to adsorption of molecules to the metal surface to create a new chemical complex. The observed SERS spectrum is a consequence of the light-matter interaction that produces transitions between vibrational energy levels. Selection rules determine which transitions are physically allowed. In traditional Raman spectroscopy, these selection rules can be derived from the symmetry point group of the molecule being studied. Interaction with a metal surface generally changes the symmetry of the adsorbate, so the selection rules involved in interpreting SERS spectra are a function of the symmetry and the spatial orientation of the adsorbate. Predicting this can be extremely difficult. Other factors that complicate SERS spectra include changes in the optical properties of the adsorbate due to plasmon resonances. One of these is obviously the large intensity increase. Interaction of the adsorbate with light, especially after the intensity enhancement, can lead to photodissociation, photoreactions, or photodesorption of the adsorbate. All of these processes leave their fingerprints in the SERS spectrum. The added complexity of all these combined effects in conjunction with a lack of reliable, reproducible nanostructures often makes interpretation of SERS spectra difficult.

2.3 References

(1) Colthup, N. B.; Daly, L. H.; Wiberley, S. E. *Introduction to Infrared and Raman Spectroscopy*; Academic Press, Inc.: New York, **1990**.

(2) Skoog, D. A.; Holler, F. J.; Crouch, S. R.; *Principles of Instrumental Analysis*; Brooks/Cole: United States, **2007**.

(3) Jenkins, F. A.; White, H. E; *Fundamentals of Optics*; McGraw-Hill: New York, **1976**.

(4) Miessler, G. L.; Tarr, D. A.; *Inorganic Chemistry*; Prentice Hall: New Jersey, **2004**.

(5) SERS review

(6) Lin, X.; Cui, Y.; Xu, Y.; Ren, B; Tian, Z.; *Analytical and Bioanalytical Chemistry* **2009**, 394, 1729-1745.

(7) Aroca, R.; *Surface-Enhanced Vibrational Spectroscopy*; John Wiley & Sons, ltd: England, **2006**.

(8) Baia, M,; Astilean, S.; Iliescu, T.; *Raman and SERS Investigations of Pharmaceuticals*; Springer: Berlin: **2008**.

(9) a new radiation

(10) papers on origin of SERS

3 Developing Experimental Techniques to Obtain Fluorescence, Raman, and SERS Spectra in Air and in Vacuum

In chapter one, the fundamentals of spectroscopy were presented. Chapter two was concerned with Raman and SERS spectroscopies. This chapter deals with the development of several techniques used to apply the spectroscopic principles presented in the previous chapters.

3.1 Binathonerator

Beginning in May 2010, the Raman spectra of a family of organic compounds called the MIDA boronate esters were collected. The effort was led by fellow honors college member Nikki Reinemann. The MIDA boronate esters were of interest to our group because of their B–N dative bonds. There has been some controversy in the literature as to the stretching frequency of these bonds due to a lack of experimental verification. This is a result of the inherent instability of many B–N containing compounds. However, the MIDA boronate esters showed good stability. The Raman spectra obtained from these compounds showed strong fluorescence that interfered with interpretation. Nikki Reinemann was able to write a computer program to subtract this fluorescence, but much of the data was distorted. I was subsequently employed to write a computer program that would manipulate Nikki's fluorescence subtracted data in such a way that pertinent information could be extracted from extraneous noise. Therefore, using National Instrument's "Labview" software, I wrote a program that would import

data points from an external file, average these points in a process called binning, graph the result, and allow the binned data points to be saved. This program was very beneficial in the analysis of the Raman data presented in the following chapter. The program allowed for importation of data from an external data file. The computer program used to collect the original Raman data provided all the data points from individuals scans in incremental column format. Based on this, the binning program was able to graph and save data for up to 32 scans. Additionally, individual scans could be included or omitted by a series of on-off switches in order to see determine their influence on the spectrum. Data could be binned by varying numbers on a control knob. The number of times the program averaged the data was determined by the number selected on the control knob. Figure 3.1a displays a screenshot of the binning program with an example spectrum distorted by noise. Figure 3.1b displays the same spectrum after being binned by 10.

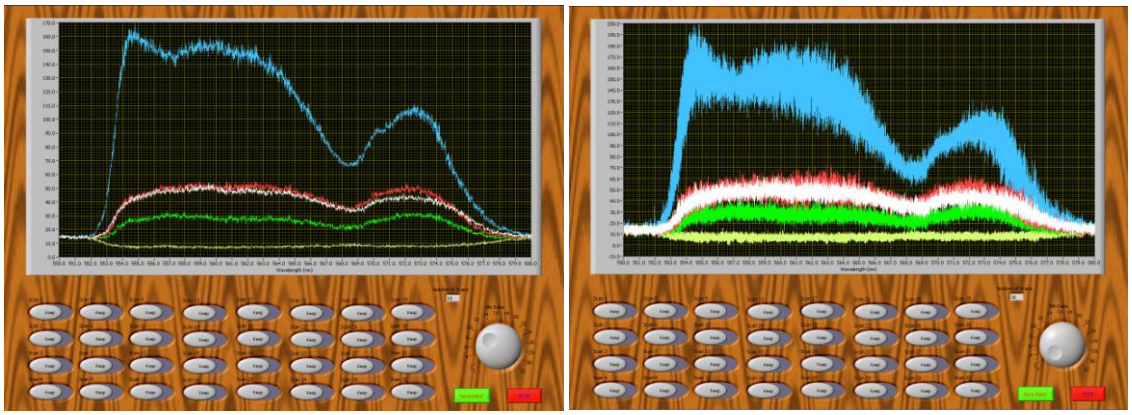

(a) (b)

Figure 3.1 a) Example spectrum distorted by noise. **b)** Example spectrum after binning by 10.

3.2 Surface Science Chamber

Surface science is the study of the interaction between two interfaces. Experimental studies of surfaces must be carefully controlled so that only the interaction of interest is observed. This is generally not possible at atmospheric pressures. A specialized vacuum chamber, often called a surface science chamber, can be used to conduct these experiments to isolate the system under study from the surrounding environment.

In the fall of 2007, Dr. Nathan Hammer's physical chemistry group at the University of Mississippi obtained a surface science chamber from storage facilities at the University of Tennessee. The chamber had been purchased in 1990 by Dr. Robert Compton of Oak Ridge Laboratories at the University of Tennessee. It was briefly used in the early 1990s to obtain data for Dr. Michael Shea's PH.D. dissertation from Vanderbilt University.

The surface science chamber consists of a massive metal housing with 17 adaptive conflat flange ports. Five of these ports are occupied by sapphire, pyrex glass, or quartz windows. Attached below the chamber are the motor, displacer assembly, and cold head of a helium cryogenic vacuum pump. The motor is connected to an external compressor by two metal high-pressure gas hoses called flexlines. Separating the cryogenic vacuum pump from the chamber is a pneumatic gate valve, allowing isolation of the cold head while it cools to working temperatures. Both the chamber and the cold head are connected to a roughing manifold by angle valves. Attached to the roughing manifold and isolated by angle valves are two liquid nitrogen-cooled cryosorption pumps

and a gas inlet. Photographs of the chamber and its accessories are shown in the following figures.

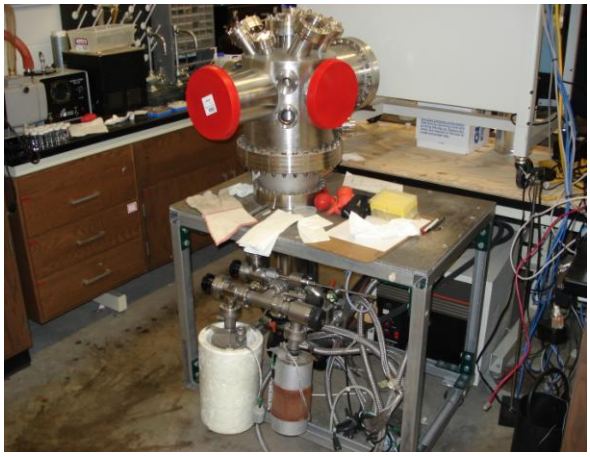

(a)

(b)

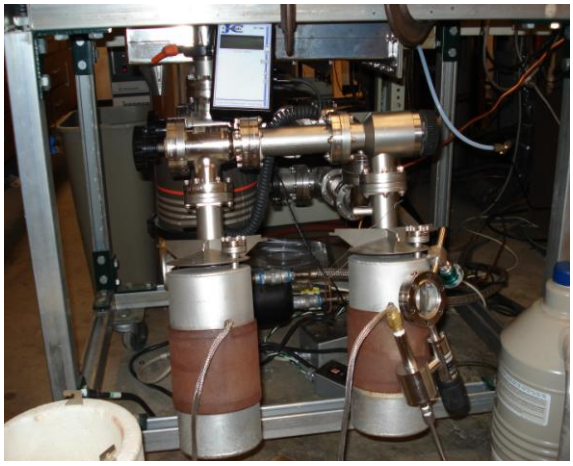

(c)

(d)

Figure 3.2 a) The surface science chamber and the stand on which it is mounted. **b)** The helium cryogenic vacuum pump mounted immediately below the chamber. **c)** Close-up of the two cryosorption roughing pumps. **d)** The external compressor of the cryogenic vacuum pump.

The cryogenic vacuum pumps associated with the chamber work by a fairly straightforward mechanism. They capture air molecules on a cooled surface by Van der Waals forces through processes called cryocondensation, cryosorption, or cryotrapping. Cryocondensation refers to condensation of gases in the air upon interaction with a very cold surface. Cryosorption can occur if molecules lose enough kinetic energy in their

interaction with a cold surface so that they adhere to that surface by Van der Waals forces. Cryotrapping is made possible with special molecular sieves that “stick” to air when cooled to low temperatures. The cleanliness of these pumping methods makes cryopumps ideal for contaminate sensitive applications such as surface science.

As mentioned, the helium cooled cryogenic vacuum pump is made up of three parts: the cold head, the motor, and the compressor. The motor works with the compressor as a refrigeration unit to cool the cold head down to very low temperatures. This is accomplished by sequentially compressing and expanding helium gas. From basic thermodynamics, gases increase in temperature when they are compressed. Conversely, gases decrease in temperature when they expand. This is easily illustrated by observing the cooling of an aerosol can after releasing its compressed contents. In the cryogenic vacuum pump, helium is first compressed in the external compressor. Afterwards, the associated increase in temperature is dissipated in a heat exchanger. The high-pressure helium is then transported to the motor unit through one of the gas flexlines. The motor provides power to a reciprocating displacer assembly that allows for efficient gas expansion. The pressurized helium entering this assembly is expanded in the cold head, cooling down two different sets of array. The working temperature for the first array is approximately 40–80 Kelvin, allowing capture of water vapor and condensation of some nitrogen gas. The working temperature for the second stage array is 11–20 Kelvin, allowing collection of nitrogen, oxygen, and argon gases. Attached to the second stage are strips of activated charcoal, which trap gases such as helium, hydrogen, and neon. After the helium gas is expanded, it is recycled back into the compressor through the return flexline and the process begins again. Consecutive cycles will cause the cold head

to become progressively colder until working temperatures are reached. Generally, an optimized setup using a helium cryogenic vacuum pump can be used to obtain ultra-high vacuum pressures.

The helium cooled cryogenic vacuum pump cannot be used to pump down the chamber directly to ultra-high vacuum pressures from atmospheric pressure. Atmospheric pressure at sea level is 760 torr. The ultra-high vacuum region begins at around 10^{-10} torr. A single helium cryogenic vacuum pump cannot accomplish this pressure change because the thermal load of such a high magnitude of gas is too large. Therefore, the chamber has to be preliminarily depressurized to around 10^{-1} torr in a process called roughing.

Two cryosorption pumps attached to the surface science chamber can accomplish this rough vacuum. Each consists of a canister filled with pellets of a substance called zeolite. Zeolite is an alumino silicate that acts as a molecular sieve to trap gas molecules. At room temperature, zeolite can trap water vapor. When cooled down to liquid nitrogen temperatures, zeolite can trap other gases such as nitrogen. A polystyrene dewar hanging from three prongs surrounds each zeolite filled canister. This dewar can be filled with liquid nitrogen, initiating the pumping mechanism.

When Dr. Hammer's group received the chamber and its parts in 2007, it had not been used since 1993. Additionally, no user manuals had been obtained for the chamber or any of its accessories. When I joined the hammer group in June 2009, no progress had been made to restore it. Being the last large nonfunctional and enigmatic instrument in the Hammer lab, it was of great interest to me. It therefore became my project to repair the chamber and its pumps, and use them to obtain high vacuum pressures.

The first step was to obtain user manuals for as many components as possible. I contacted Varian, the company that made the helium cryogenic vacuum pump. They informed me that they had discontinued production of cryogenic pumps a decade ago, and the rights to all previously manufactured products of this nature had been sold to a company called Ebara. My attempts to obtain a user manual from Ebara and several other companies proved unsuccessful. Exhaustive Internet searches for a user manual to any Varian cryogenic vacuum pump provided similar results; that type of vacuum system apparently had its prime before the digital age. Similarly, the company that made the liquid nitrogen cooled cryosorption pumps had discontinued production of the models we possessed. They did still have product information available online, so I was able to secure an operating procedure for these pumps.

My goal became to learn the general theory of operation for helium cryopumps, and to try to apply this knowledge to our instruments. I obtained user manuals for several modern helium cryogenic pumps. From these I determined that the first step in my restoration of this equipment should be to charge the compressor and the gas flex lines with helium, and purge out any unwanted contamination. We purchased an ultra high purity helium gas cylinder and a high-pressure regulator, and had a special tool called a maintenance manifold custom made that could couple the helium tank to the flexlines and the compressor. The compressor and the flexlines had various leaks that impeded progress. Also, there was some uncertainty as to what pressure the flexlines and the compressor should be charged to. A rough estimate was made based on the pressure specifications of similar cryogenic pumps, and the maintenance manifold was used to charge the compressor and the flexlines to this pressure.

Concurrently, the status of the cryosorption roughing pumps was determined. In order to test the roughing pumps, the surface science chamber had to be appropriately sealed by replacing several gaskets and flanges. We were able to borrow liquid nitrogen from various professors in the University of Mississippi Chemistry Department. The cryosorption pumps were then activated by the addition of liquid nitrogen. We determined that one of roughing pump and its associated angle valve had significant leaks, and could not be salvaged. The other roughing pump was in perfect condition. Using just the one cryopump, we were able to reduce the pressure in the chamber to less than 10 mtorr.

The next step was to determine if the electrical connections on the motor/displacer assembly and compressor of the helium cryogenic pump worked. The easiest way to accomplish this was to try and turn the pump on. Temporary water and electrical lines were connected to the compressor. The chamber and the cold head were then roughed out, and the compressor was turned on. Both the compressor and the motor appeared to be in working order. Permanent electrical connections were then installed by the University of Mississippi physical plant. Similar permanent water connections were stinted from an existing water main in the lab.

By July 2009, all necessary precautions had been taken, and the helium cryogenic pump was ready to be opened to the chamber. The chamber and the cold head were roughed down to approximately 10 mtorr, and the helium cryogenic pump was turned on. The cold head took approximately four hours to cool down to the appropriate temperature, as given by an attached temperature gauge. A nitrogen gas tank was used to open the pneumatic gate valve after cooling. The pressure in the chamber, as measured by

an XXX ion gauge, was approximately $1*10^{-4}$ torr, seven orders of magnitude lower than atmospheric pressure.

3.3 Development of Fluorescence Setup in Vacuum

It was necessary to find a use for the surface science chamber that was relevant to the interests of our laboratory. The first application of this chamber was for obtaining fluorescence spectra in vacuum. This was significant because all substances interact with the air around them at atmospheric pressure. In some cases, these interactions can lead to detectable changes in any collected spectroscopic data. Removing much of the surrounding air when collecting data allows these interactions to be minimized. The substances effectively become isolated, making the contribution of air to collected spectroscopic data negligible. The first step was to figure out how to collect the luminescence from inside the sealed vacuum chamber. We purchased a high-vacuum fiber optic cable and a conflat fiber optic adaptive flange from Ocean Optics. The specially made material of the cable allowed collection of light from inside the chamber at high vacuum pressures. The conflat fiber optic adaptive flange was mounted on the surface science chamber to couple the internal high vacuum fiber optic to an external fiber optic cable, which then transported the collected light to a CCD camera type detector. The next step was to find a sample holder that we could use to position both the sample of interest and the internal fiber optic cable. We made such a sample holder using a flat piece of metal with a hole drilled in it and a metal clip. A photograph of the sample holder, fiber optic cable, and focusing lens is shown in figure 3.3.

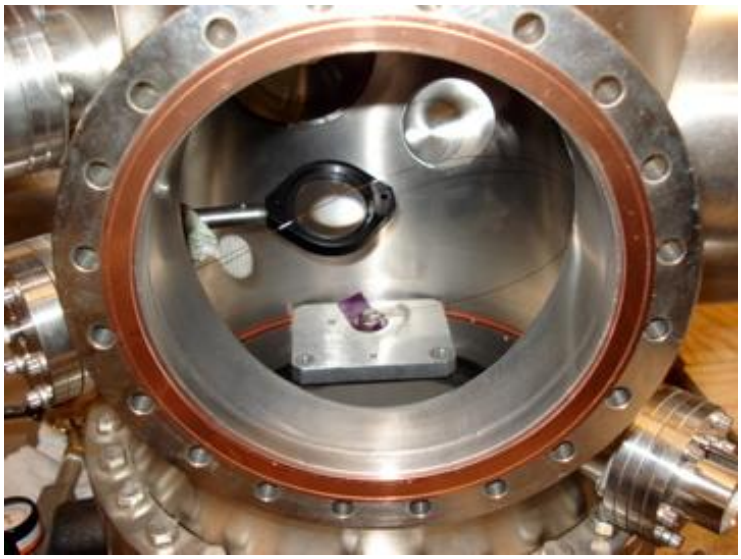

Figure 3.3 The inside of the surface science chamber containing the lens, high vacuum fiber optic cable, sample chamber, and a sample used to obtain fluorescence spectra in vacuum.

Xenon arc lamps produce highly intense light in visible and ultraviolet regions of the electromagnetic spectrum, making them excellent light sources for fluorescence spectroscopy. The Hammer Group possesses a number of these lamps and one of these lamps and its power supply were assembled adjacent to the surface science chamber. A small Instruments SA. Inc. grating monochromator was used to select the various wavelengths of interest. The windows on the surface science chamber were not of the appropriate angle to allow the light from the Xenon Arc lamp to fall directly on the sample holder, so focusing mirrors were used to manipulate the light beam to the right position. Due to the divergence of the beam, a long focal length lens was placed in front of the window mount. A short focal length lens was placed inside the chamber to further focus the light to a tiny point on the sample holder.

3.4 Development of Surface Enhanced Raman Scattering (SERS) Spectroscopy in Vacuum

At the very beginning of my laboratory research, my main goal was to develop the technique to perform Raman spectroscopy experiments inside the surface science

chamber under vacuum. However, we soon discovered that the development of this technique would be trivial. Given the renewed interest in SERS spectroscopy after the discovery of a single molecule in 1997, optimization of a SERS spectroscopy setup in vacuum seemed like a worthy goal. SERS provided more extensive applicability than traditional Raman spectroscopy. Also, superficially, the "surface" science chamber seemed destined for a "surface" sensitive application.

The method of SERS substrate creation had to be determined. Given our unique interest in producing SERS spectra in vacuum, the chosen substrate had to be able to accommodate the rigors of the pump down cycle. The method also had to be feasible given the limited amount of equipment we had access to. Colloid suspensions were of initial interest due to their low cost of production and no need for special equipment. The basic idea was to make the colloid suspensions in a volatile solvent, add the desired analyte, and deposit the result onto a glass slide. After evaporation of the solvent, the slides could be analyzed. Due to the ambiguities of depositing the suspension on a slide, the composition of the substrate could not be very well controlled. Thus, this method would not have been ideal. The substrate problem solved itself in December 2009 when chairman of the chemistry department Dr. Charles Hussey informed our group that he had a vacuum deposition chamber, which was not being used.

Vapor deposition of metals onto silicon, glass, or graphite slides is a well-known technique used to produce metal island films. As mentioned in chapter 2, the composition of the deposited substrate can be controlled by varying deposition rates, deposition amounts, and slide temperature. Highly SERS active and air stable substrates can be produced. This method also allowed fairly easy integration of SERS with the surface

science chamber, because the substrates would not have to be altered during the pump down process.

We acquired an Edwards vacuum deposition chamber known as the AUTO 306. The AUTO 306 is described in the user manual as “a microprocessor controlled vacuum coater than can be configured to perform a variety of coating tasks”. It consists of a vacuum pumping system, a microprocessor control system and control panel, a baseplate, an electrical system, and a cabinet. A large bell jar and implosion guard contain the baseplate and the vapor deposition equipment. Figure 3.4 show photographs of the chamber and the vacuum pumps.

(a)

(b)

(c)

(d)

Figure 3.4 a) The vacuum deposition chamber. **b)** Close-up of the bell jar and implosion guard containing the vapor deposition equipment. **c)** The rotary pump and the oil diffusion pump contained in the cabinet below the bell jar. **d)** The front panel of the microprocessor control system and the quartz crystal microbalance display.

In order to begin the deposition process, the vacuum system must bring the chamber to working pressures through the use of two vacuum pumps. A rotary vacuum pump brings the chamber down to rough vacuum, at which point, an oil diffusion pump is activated to bring the chamber down to pressures lower than 1×10^{-7} torr. The purpose of the vacuum system is to create an environment inside the chamber such that solid materials will sublime when heated. Once removed from the heating source, the created vapor is free to travel around and deposit itself on to any available surface as it cools. The materials deposited in these types of chambers are generally metals. The sublimation process begins by wrapping a small amount of wire made of the material to be deposited around a tungsten coil. The tungsten coil is then inserted into an electrical system. Current is passed through the coil, and resistive heating of both the coil and the deposition material occurs. The temperature of the coil can be controlled by varying the magnitude of the current.

Implanted inside the chamber is a Sycon STM-100 quartz crystal microbalance. This accessory is able to monitor deposition amounts and deposition rates. The quartz crystal microbalance works by passing a small amount of electricity through a piezoelectric substance such as a quartz crystal. Piezoelectric is a term used to describe substances that vibrate in response to current. The frequency of vibration is a function of several properties of the substance, including its mass. Thus, small differences in the mass of the crystal can be detected by monitoring the frequency of its vibration.

The AUTO 306 deposition chamber combined with the quartz crystal microbalance was a perfect instrument to make SERS active metal island films. Silver was selected to be the deposition metal because of its common use in SERS literature and because of its very high enhancement capabilities for excitation sources in the visible region of the electromagnetic spectrum. 1.5″x1″x1mm glass slides were cleaned by successive washing in concentrated hydrochloric acid, deionized water, and ethanol, and blown dry with nitrogen. Each slide was placed in a Harrick Plasma PDC-32G plasma cleaner to remove any surface impurities. The slides were then positioned on the baseplate of the AUTO 306. The AUTO 306 was kept at a pressure of approximately 1 x 10^6 torr during deposition. A thin oxide coating was likely formed on each slide due to the brief trip in atmosphere from the plasma cleaner to the deposition chamber. Silver was deposited on the slides at a rate of 0.02 nm/s to until a total coverage of 7 nm was reached.

The SERS activity of the films needed to be tested. This was possible by using the molecule Rhodamine 6G. Rhodamine 6G is an organic dye that strongly fluoresces when interacting with light in the visible region of the electromagnetic spectrum. The low intensity Raman scattered light cannot be distinguished from a strong fluorescence background. Thus, an ordinary Raman spectrum cannot be readily obtained for Rhodamine 6G using Raman setups that utilize visible laser lines. The unique properties of SERS active substrates often allow fluorescence to be quenched, making a SERS spectrum of Rhodamine 6G attainable. Rhodamine 6G is frequently used in the literature to determine the quality of new SERS substrate production techniques. Consequently, we

were able to verify the quality of our own SERS substrates produced using the AUTO 306 by taking SERS spectra of Rhodamine 6G.

A 10^{-4} M solution of Rhodamine 6G in ethanol was prepared. The concentration of this solution is far below the detection limit for normal Raman spectroscopy of 0.1 M. The Rhodamine solution was added to a SERS substrate using the "drop method". This simple method requires a drop or two of the sample solution to be placed onto a SERS substrate. Upon evaporation of the solvent, the SERS spectrum of the analyte can be taken. The SERS spectra were taken using the microscope setup on a restored Jobin-Yvon Ramanor HG2-S Raman Spectrometer updated with a modern computer control and data acquisition system. The restoration was accomplished between 2007 and 2009 by former honors college graduate Austin Howard. This experimental setup utilizes a Coherent Innova Argon Ion Laser as the excitation source. The laser line interacts with a sample in a chamber attached to the Ramanor, and light is collected and processed by the Ramanor itself. Using the 514.5 nm line of the Argon laser and this setup, the position of the SERS substrate was optimized for data collection. Figure 3.5a shows the spectrum obtained from the substrate. Without varying any experimental parameters, the Rhodamine 6G solution was deposited on the SERS substrate and the spectrum was taken again. The SERS spectrum of Rhodamine taken by this method is shown in figure 3.5b.

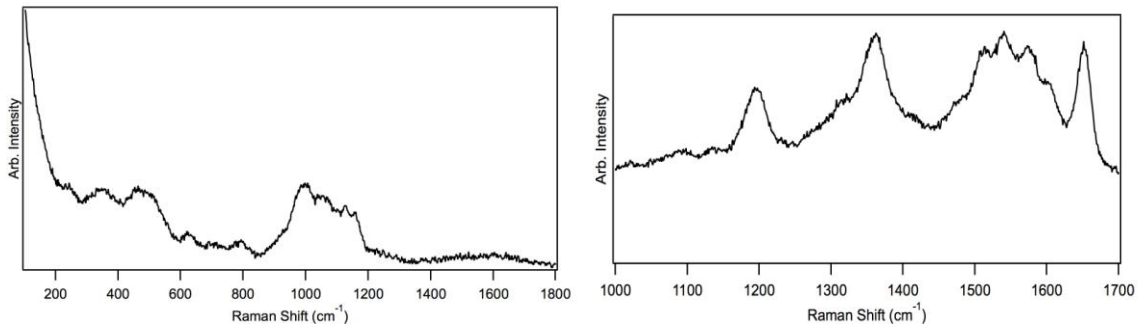

(a) (b)

Figure 3.5 a) Spectrum of SERS substrate before addition of Rhodamine 6G. **b)** SERS spectrum of Rhodamine 6G.

The SERS spectrum of Rhodamine 6G shows clearly discernable peaks at 600 cm^{-1}, 764 cm^{-1}, 1185 cm^{-1}, 1343 cm^{-1}, 1553 cm^{-1}, and 1622 cm^{-1}. The presence of peaks and the lack of the fluorescence background provided qualitative assurance that the SERS effect had worked to quench the fluorescent tendency of Rhodamine 6G. The spectrum of Rhodamine 6G obtained from the Ramanor setup was very similar to a recently published SERS spectrum of Rhodamine 6G on a vapor deposited substrate[0]. Both spectra shown in figures 3.5a and 3.5b show peaks at 1185 cm^{-1}, 1343 cm^{-1}, 1553 cm^{-1}, and 1622 cm^{-1}. The two spectra are not identical, but due to the difficulties in reproducing SERS data this is to be expected. The relative intensity of the peak at 1622 cm^{-1} shown in figure 3.5b is smaller than the corresponding peak in figure 3.5a. The difference can be attributed to dissimilarities in substrate composition or to slightly altered geometries of the adsorbed Rhodamine 6G molecule on the silver surface.

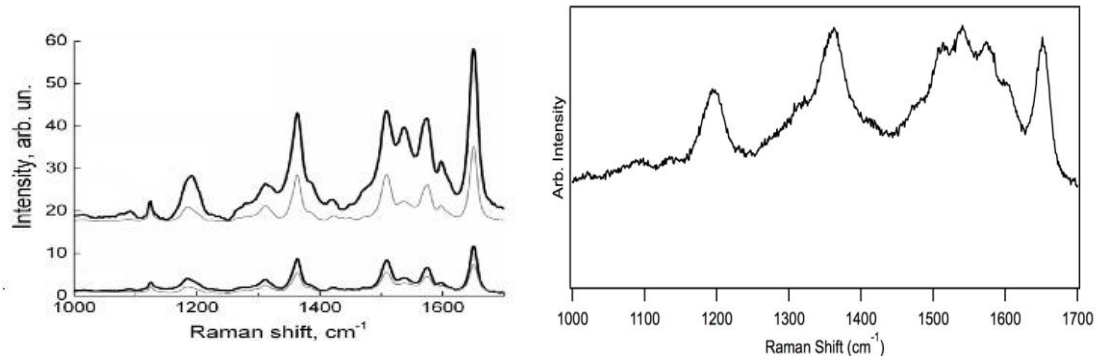

(a) (b)

Figure 3.6 a) SERS spectra of Rhodamine 6G from Reference X **b)** SERS spectrum of Rhodamine 6G using the restored Ramanor HG2-S

By obtaining the SERS spectra of Rhodamine 6G and comparing it to the literature, we were able to demonstrate that our substrates showed SERS activity of publication quality. The new goal became to use these SERS substrates to obtain a spectrum of Rhodamine 6G in vacuum. Utilizing the setup to obtain fluorescence data described previously, the transition of SERS from air to the vacuum chamber was relatively simple. The Rhodamine 6G was added to a SERS substrate via the drop method. This substrate was then placed inside the surface science chamber in the sample holder developed for fluorescent samples. The 514.5 nm laser line of a Coherent Innova Argon Ion laser was manipulated with mirrors to shine through a window on to the sample. Two lenses were used to focus the light down to a point. The Raman signal was collected with a fiber optics cables and transmitted to an Princeton Instruments Acton SP2500 spectrograph and a XXX CCD camera type detector. A 514.5 nm notch filter was placed inside the spectrograph housing. The photograph of the laser light entering the surface science chamber is shown if figure 3.7.

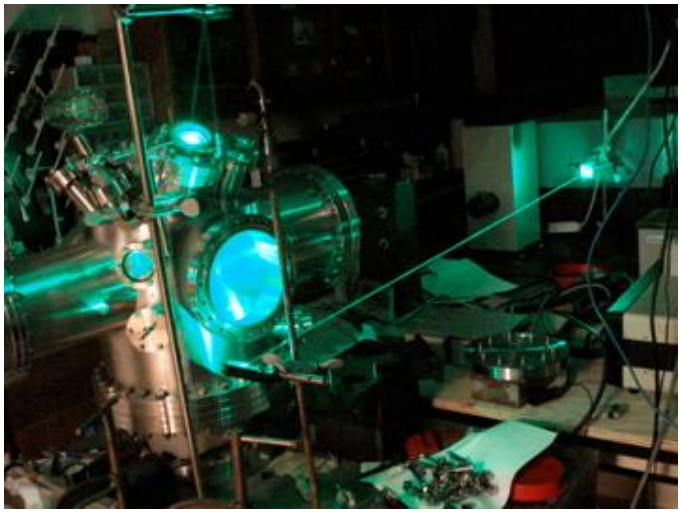

Figure 3.7 shows the 514.5 nm laser line from an Argon laser reflecting off a series of mirrors and entering the surface science chamber. This setup was used to obtain SERS spectra of molecules in vacuum.

Using this experimental setup we were able to obtain SERS spectra for Rhodamine 6G in vacuum. Due to time constraints, the helium cryogenic vacuum pump could not be turned

on. However, rough vacuum was obtained using the cryosorption vacuum pump. A spectrum taken using this setup is shown in figure 3.8.

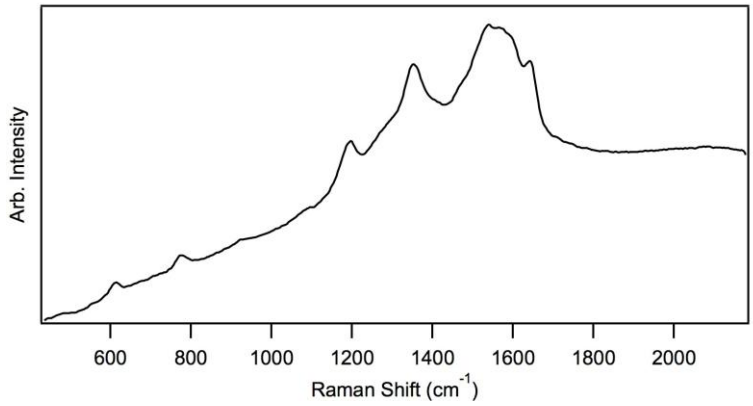

Figure 3.8 SERS spectrum of Rhodamine 6G in obtained in vacuum

The spectrum of Rhodamine 6G taken in vacuum retains the characteristic peaks at 600 cm^{-1}, 764 cm^{-1}, 1185 cm^{-1}, 1343 cm^{-1}, 1553 cm^{-1}, and 1622 cm^{-1}. The relative intensities of the peaks appear to have changed quite drastically. This could be due frequency shifted laser light scattered off the multiple mirrors and lenses used in the experimental setup. The frequency-shifted light could then interact with the local surface plasmons in the SERS substrate to produce an enhancement that convoluted the desired spectrum. A notch filter placed in a better location than inside the spectrograph could reduce this unwanted radiation. Figure 3.8 depicts a classical example of what is known as the SERS continuum: the sloping baseline that appears in many SERS spectra.

3.5 References

(1) Reference that you got spectra from

(2) Users guide to vacuum technology

(3) Sumitomo cryogenic vacuum user manual

(4) SERS continuum paper

4 Fluorescence and SERS Investigation of Organic Molecules

The following chapter provides data that illustrates practical applications for the spectroscopic techniques developed and described in chapter 3. Fluorescence spectra were obtained in air and in vacuum for a family of new organometallic molecules in order to determine their possible use in industry. SERS spectra were obtained in air and in vacuum for a family of boron nitride containing molecules in order to assign a value to the stretching frequency of the B–N dative bond.

4.1 Fluorescence Spectra of Organometallic Molecules

Metals and metal containing compounds have been known to catalyze organic reactions. One widely known metal catalyst is palladium, which catalyzes the hydrogenation of alkenes and alkynes. In XXXXX the research group of Dr. Keith Hollis at the University of Mississippi began synthesizing organometallic compounds for the purpose of catalyzing hydroamination reactions. Hydroamination reactions refer to the direct addition of ammonia, a primary amine, or a secondary amine to an alkene or an alkyne. These reactions are extremely important to organic chemistry because they offer a pathway to create amines, enamines, and imines with 100% theoretical efficiency. In the quest to create an effective catalyst for hydroamination reactions, several compounds were produced with the following structural skeleton.

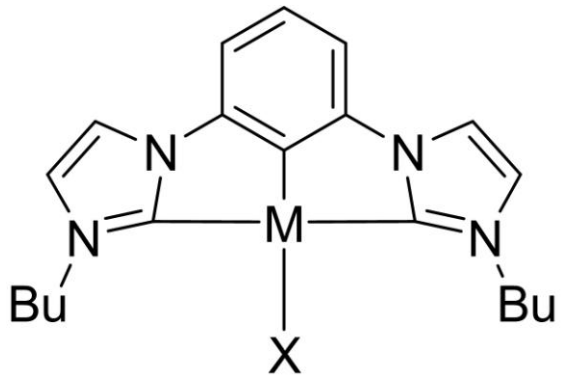

Figure 4.1 shows a lewis structure skeleton of the organometallic molecules synthesized by the Hollis group at the University of Mississippi.
M = Pt, Rh
X = Cl, Br

The newly synthesized compounds unfortunately did not exhibit the desired catalytic activity. However, upon characterization, it was discovered that they produced strong fluorescence in the blue region of the electromagnetic spectrum. As mentioned in chapter one, fluorescence is a type of spontaneous emission that occurs when a chemical species in an electronic excited state relaxes to the ground state. The blue emitting compounds thus had great potential for industrial use in organic light emitting diodes (OLEDs).

Light emitting diodes (LEDs) are generally doped inorganic semiconducting substances that produce light in response to current. Light emitting diodes have been of industrial importance since 1929, when a Russian scientist named Oleg Losev developed a light array for communication purposes. The technology has since expanded rapidly, challenging traditional light sources such as incandescent, halogen, and fluorescent lights. In many cases, LEDs can offer lower operating costs, and better reliability and performance than traditional sources. LEDs have the ability to only produce light of the desired emission color, enabling them to use less energy in comparison with filtered light from a white source. Innumerable applications for LEDs include computers, televisions, street lamps, holiday lights, and exit signs.

A limitation to LED technology is the high cost factor in producing large quantities of doped semiconductors. Semiconductor materials are coveted due their widespread use in electronic circuit boards. Additionally, silicon, germanium, aluminum, and other materials used in the production of semiconductors must be mined and purified before use. Consequently, technological advancements in electronics and competition among industries have led a dramatic increase in the price of starting materials. One way to circumvent this problem is to use organic molecules. Specially made organic materials can produce light in response to current, acting as organic light emitting diodes. OLEDs, though younger than their counterpart LEDs, have found their way into a huge variety of applications, and further developing the area is a hot topic of research.

Considerations when developing molecules suitable for use in OLEDs include the cost of production, the color of the emitted light, the stability of the organic molecule, and the energy efficiency. The color of the emitted light, the stability of the molecule, and in some cases the energy efficiency can be assessed using fluorescence spectroscopy. In an actual OLED, electricity is used to excite the organic molecules to higher energy levels. But in the initial characterization process, the electric stimulus can be simulated by using light. Fluorescence data is cheap and easy to obtain and is useful in order to determine if the molecule is worth a more serious evaluation.

Fluorescence spectra were collected for the organometallic molecules discussed above. The fluorescence setup inside the surface science chamber discussed in chapter 3 was used to collect all spectra. The excitation wavelength for each analysis was 365 nm. The following spectra were taken at atmospheric pressure.

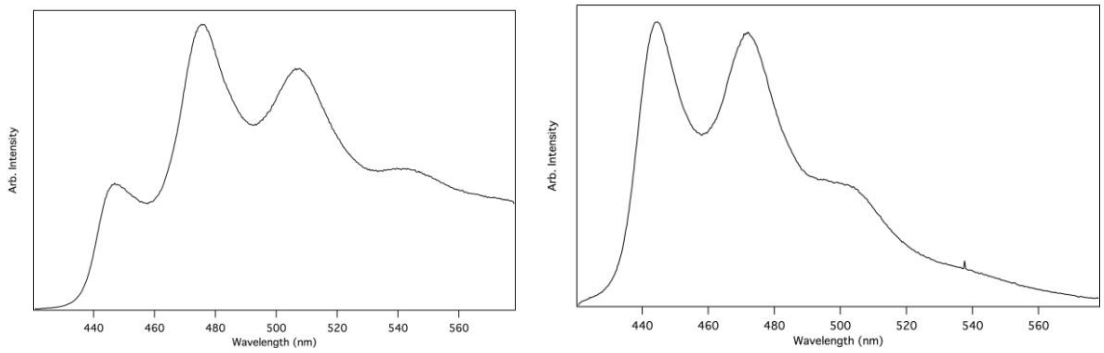

(a) (b)

Figure 4.2 a) The fluorescence spectrum of XXXX in air **b)** The fluorescence setup of XXXXX in air

Figure 4.2a showed prominent peaks at 446 nm, 474 nm, and 506 nm. Figure 3.2b showed prominent peaks at 443 nm and 471 nm and a slight peak at 504 nm. The stability of these compounds in air appeared to be at least 95% over 6 hours of data accumulation. Spectra of these compounds in vacuum were also taken in order to assess interactions with air that may influence the observed spectra. The following spectra were taken in the surface science chamber at 20 mtorr using an excitation wavelength of 365 nm.

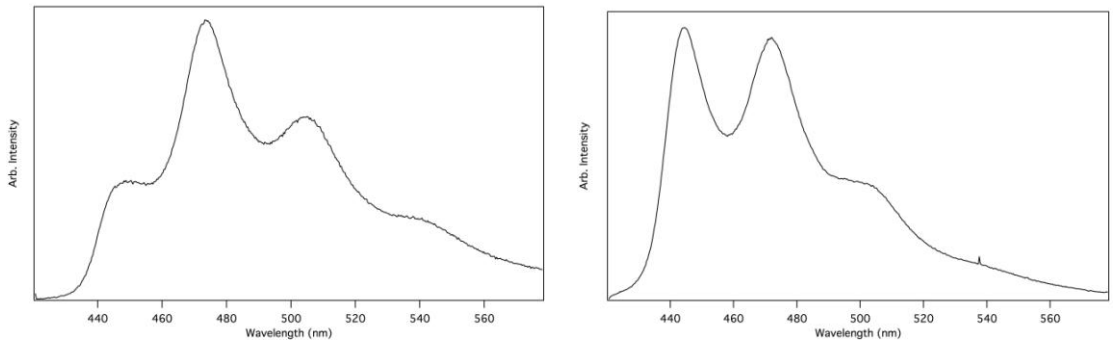

(a) (b)

Figure 4.3 a) The fluorescence spectrum of XXXX in vacuum **b)** The fluorescence spectrum of XXXX in vacuum

Neither spectrum changed in the absence of air. This was expected. Compounds exposed to air and light for long periods of time generally do not change when subjected to vacuum pressures. A more conclusive investigation of the effects of the air on each of

these compounds could be accomplished by synthesizing each in the absence off one or more components of air and/or in the absence of light. The fluorescence spectra of these molecules could then be monitored in vacuum, or during the addition of air.

Each compound was thought to undergo a ligand exchange reaction with carbon monoxide. The surface science chamber, having been evacuated was then refilled with pure carbon monoxide in order to determine the influence carbon monoxide on the collected fluorescence data. The following spectra were taken with the chamber filled with XXX pressure of carbon monoxide after the given length of time.

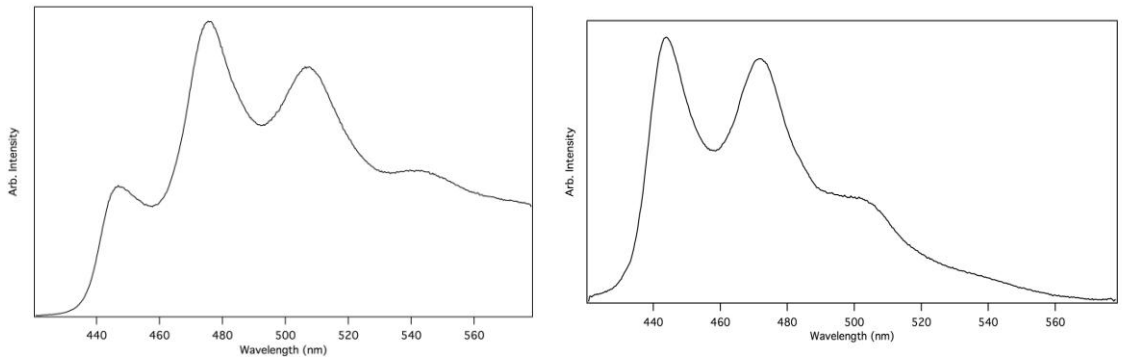

(a) (b)

Figure 4.4 a) The fluorescence spectrum of XXXX after subjection to carbon monoxide for 36 hours **b)** The fluorescence spectrum of XXXX after subjection to carbon monoxide for 12 hours

The position of the peaks in figures 3.4a and 3.4b did not shift due to the influence of carbon monoxide. However, the true effect of carbon monoxide on each compound cannot be readily determined by viewing a two-dimensional plot. If ligand exchange did occur, there should be a corresponding reduction in the relative intensity of one or more peaks as the compound changed. Therefore, the relative intensity of the peaks shown in figure 4.4a was measured over a ten-minute increment during the addition of carbon monoxide to the chamber. The intensity of each peak declined significantly during this period. A waterfall plot showing the results is given in figure 4.5.

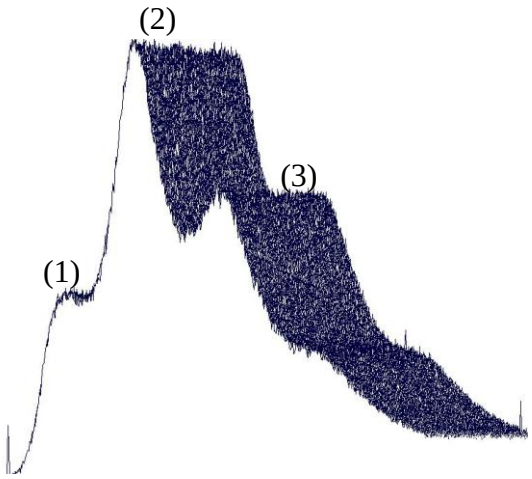

Figure 4.5 shows the fluorescence spectra of XXXXX over a ten minute period while subjected to a carbon monoxide rich environment.

The peaks at 446 nm, 474 nm, and 506 nm correspond to peaks (1), (2), and (3) in the waterfall plot shown in figure 4.5 respectively. The relative intensity of peak (1) decreased by 30 percent over the ten-minute period. The relative intensity of peak (2) decreased by 2 percent. The relative intensity of peak (3) decreased by 5 percent. The marked reduction in the intensity of each peak, especially in peak (1), suggests that XXXXX participated in a ligand exchange reaction with carbon monoxide.

4.2 SERS Spectra of Boronic Acid MIDA Esters

As briefly introduced in chapter 3, in May 2010, Dr. Nathan Hammer's research group at the University of Mississippi began studying boronic acid MIDA esters. The project was led by fellow honors college member Nikki Reinemann. The family of boronic acid MIDA esters was of interest to our group due to their boron nitrogen dative bonds.

Bonding in molecules can be ionic or covalent. Ionic bonds exist when the electron distribution between two atoms is very unequal. One atom accepts electrons to become negatively charged, while the other loses electrons to become positively charged. The result is two atoms effectively bonded by electrostatic forces. In a covalent bond, the electron density of the bond is distributed fairly equally between two atoms. Each atom is

independently attracted to the shared electrons. If the covalent bond is formed as a result of unequal electron contribution from the bonded atoms, the result is a coordinate covalent bond, or a *dative bond*. Although the resulting bond is indistinguishable from other covalent bonds, the chemistry of the reaction that created the bond is different.

Dative bonds containing boron atoms have been studied for many years. In particular, donor-acceptor complexes involving B–N dative bonds have been known for more than 100 years and have been investigated extensively since G.N. Lewis proposed his revolutionary theory on acids and bases. The strength of these bonds greatly varies depending on the substituents attached to both the boron and nitrogen atoms. Assignment of a vibrational frequency to this bond has been particularly elusive, with values ranging from 500 cm^{-1} to 1200 cm^{-1}. Each of these previous assignments has been primarily based on theoretical calculations. The inherent instability of B–N dative bond containing complexes has made experimental verification impossible in many cases.

One well-studied family of molecules is the boronic acids. Interest in boronic acid functional groups has blossomed due to their use in pharmaceuticals. Various boron-containing derivatives can also be prepared from these compounds that also have physiological effects. However, boronic acids have a troubling tendency to decompose in air by photodeboronation, oxidation or polymerization. However, boronic acids complexed with a trivalent ligand called N-methyliminodiacetic acid (MIDA) have been found to air stable indefinitely.

Methylboronic acid MIDA ester and naphthylboronic acid MIDA ester were used in this study due to their stability in air. These are new molecules, recently marketed, that

have never been investigated by vibrational spectroscopic methods. The structures of these molecules are shown in figure 4.X.

Despite their stability, initial Raman studies of methylboronic acid MIDA ester and naphthylboronic acid MIDA ester by Reinemann proved frustratingly inconclusive due to the strong observed fluorescence of these molecules. As mentioned in chapter 2, the excitation frequency used in Raman spectroscopy is not important as long is absorption is not promoted. Although excitation with frequencies that closely approach an electronic absorption band is premise for Resonance Raman Spectroscopy, if strong absorption actually occurs, relaxation in the form of fluorescence convolutes the spectrum such that individual peaks cannot be distinguished from the background. The 514.5 nm line of the ion argon laser promoted absorption in both MIDA ester compounds studied. The original spectrum taken of methylboronic acid MIDA ester is shown in figure 4.X

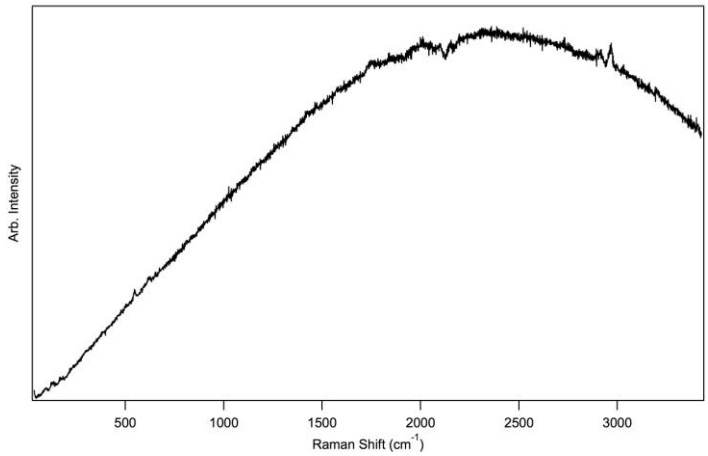

Figure 4.X shows the unmodified Raman spectrum of methylboronic acid MIDA ester as taken with the 514.5 nm line of the argon ion laser.

The spectrum shown in figure 4.X shows the how fluorescence can make the identification of Raman shifted peaks nearly impossible. A few tiny peaks are apparent in the spectrum, but their intensity relative to the fluorescence background is so low that they cannot be correlated to vibrational modes with much confidence.

Despite the initial setbacks, Reinemann took Raman data of these compounds in small increments over a long period of time. She then wrote a computer program to subtract fluorescence from a conglomeration of this data. Additionally, she used the Binathonerator program introduced in chapter 3 to average the data. The resulting spectra showed fairly well resolved peaks, from which the peak corresponding to the B–N stretching mode could be identified for each compound, making the overall effort a success.

After development of the SERS technique, and the success in obtaining SERS spectra from Rhodamine 6G, the Hammer group began looking for other molecules to study. The MIDA ester compounds soon became the obvious choice as a proof of principle exercise illustrating the fluorescence quenching properties of the SERS active substrates. Additionally, this application provided valuable data to the Hammer group useful when publishing the research obtained on B–N stretching frequencies.

The fluorescence quenching ability of SERS active substrates has been known since SERS frenzy of the 1980s. Yet, while it is true that SERS substrates can quench fluorescence in some cases, the effect is not simplistic and does not always happen. Fluorescence enhancement can also occur. The mechanism of fluorescence modulation is attributed to interaction of the adsorbate with the metal surface. The effect of the metal surface on fluorescence is highly dependent upon the quantum efficiency of the adsorbate. Quantum efficiency is simply the ratio of the number molecules that fluoresce, to the number of molecules that are in an excited state. As mentioned in chapter one, relaxation to the ground state can occur in the form of radiative or nonradiative transitions. Nonradiative transitions are responsible for quantum efficiencies less than

unity. If the quantum efficiency of the analyte is *initially high*, approaching unity, coupling of the molecule to plasmon resonances of the SERS substrate will create an additional nonradiative decay channel for the excited state species. This additional channel leads to a reduction in quantum efficiency and the corresponding fluorescence intensity is strongly *diminished*, or quenched. Inversely, if the quantum efficiency of the adsorbate is *initially very low*, the fluorescence intensity can be *enhanced* by a similar mechanism. Such enhancements are generally limited to a factor of approximately 10. Many factors affect the quantum efficiency of a given molecule, including changes in structure, temperature, or concentration. Therefore optimizing the fluorescence quenching in SERS tends to be a capricious process. The amount of coverage of the adsorbate on the SERS substrate, i.e. the concentration of the solution applied when using the drop method, seems to be the most widely tuned variable.

All SERS active substrates created to study methylboronic acid MIDA ester and naphthylboronic acid MIDA ester were fabricated using the AUTO 306 vacuum deposition chamber described previously. Pressures in the deposition chamber were approximately 1×10^{6} torr throughout the deposition process. Clean glass slides were coated with silver to 7 nm at a deposition rate of 0.02 nm/s.

Methylboronic acid MIDA ester and naphthylboronic acid MIDA ester were deposited on the SERS active substrates via the drop method described previously. In each case, the solvent used had a profound effect on the observed SERS spectrum. SERS spectra were taken using the 514.5 nm line of a Coherent Innova Ion Argon Laser providing 1 watt of power. The microRaman setup of the previously mentioned restored

Jobin-Yvon Ramanor HG2-S Raman Spectrometer was used to collect and analyze the scattered light.

Methanol was originally used as the solvent when making a solution of methyboronic acid MIDA ester to drop coat on the SERS substrate. The SERS spectra taken using methanol as the solvent showed no significant peaks. In fact, the observed spectra looked suspiciously similar to the spectrum of the SERS substrate alone shown in figure 3.5a. Despite varying the concentration of methyboronic acid MIDA ester in methanol, all spectra looked similar to figure 4.X, which shows the spectrum of a substrate coated using a high concentration of methylboronic acid MIDA ester in methanol.

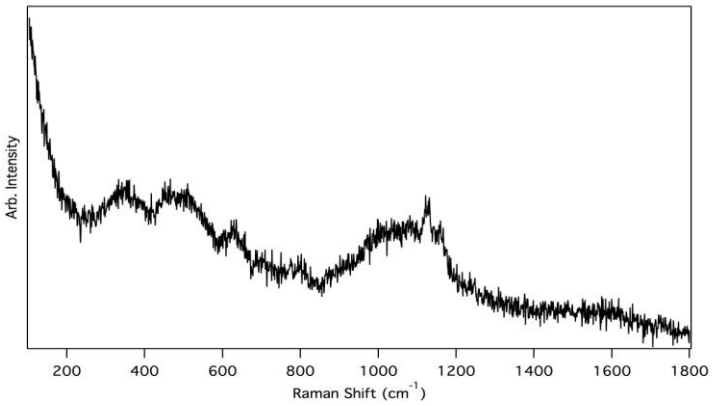

Figure 4.X shows a typical SERS spectrum obtained from drop coating methylboronic acid MIDA ester dissolved in methanol.

Acetone was then chosen to be the solvent in the SERS studies of methylboronic acid MIDA ester. The results were immediately better. The ability of the solvent to affect the observed SERS spectrum was an additional consideration when producing SERS spectra. Solvent molecules vigorously attracted to the SERS substrate can displace the analyte of interest. Complexes between analyte and solvent may not adsorb at all. The inverse is true; analytes that have trouble adsorbing to a surface may benefit from a coordinating solvent. Whichever the case, methylboronic acid MIDA ester dissolved in

acetone provided a much better SERS spectrum than methylboronic acid MIDA ester dissolved in methanol as demonstrated by comparing figure 4.X to figure 4.X.

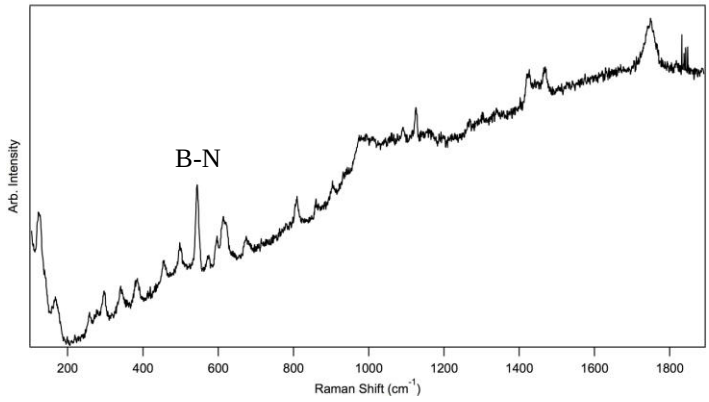

Figure 4.X shows the SERS spectrum obtained from drop coating methylboronic acid MIDA ester dissolved in acetone.

The prominent peaks present in figure 4.X indicate that fluorescence has been quenched to some extent, implying that the SERS effect is working. The spectrum also shows another example of the SERS continuum, the sloping baseline present in many SERS spectra. The continuum could be easily subtracted. However, recent studies suggest the continuum may be of physical importance, arising from surface-enhanced fluorescence.

In order to determine which peak in the spectrum corresponded to the stretching mode of the B–N dative bond, the spectrum displayed in figure 4.X was compared to theory and to the modified Raman spectrum of methylboronic acid MIDA ester, both provided by Reinemann. Figure 4.X shows a comparison of the three spectra.

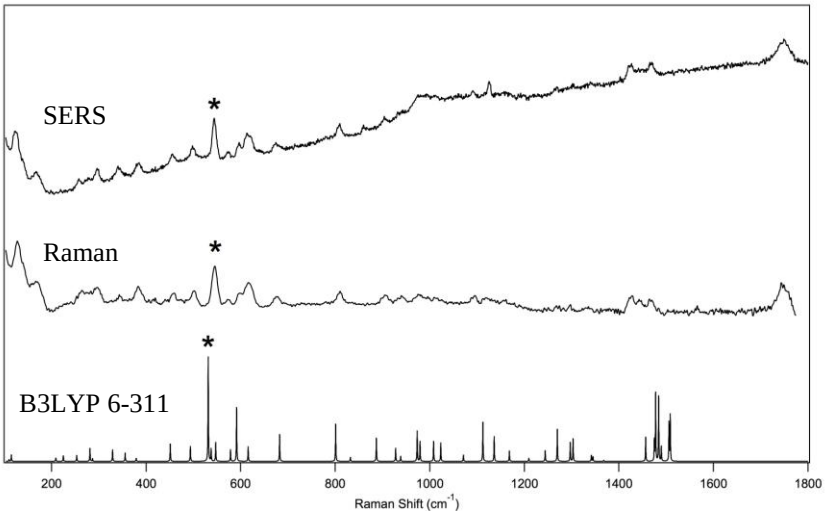

Figure 4.X shows the SERS and Raman spectra of methylboronic acid MIDA ester as compared theory from the B3LYP 6-311+G 2df basis set.

The peaks in the modified Raman spectrum and the spectrum produced using the B3LYP 6-311+G 2df basis set correlated well with the peaks in the SERS spectrum. The similarities suggested methylboronic acid MIDA ester was physisorbed to the SERS substrate. Had the methylboronic acid MIDA ester been chemisorbed to the SERS substrate, peaks in the spectrum would have appeared, disappeared, or have been shifted to do the formation of the new complex. The prominent peak at approximately 545 cm^{-1} indicated in each spectrum by a star was assigned as the stretching frequency of the B–N dative bond. Ultimately, both the SERS and modified Raman spectra of methylboronic acid MIDA ester looked strikingly similar and gave the same value for the stretching frequency of B–N dative bond. However, as mentioned previously, the data used to produce the Raman spectrum shown in figure 4.X was taken over the course of several months by integrating hundreds of scans of small regions and splicing them together. Modification to the Raman spectrum of methylboronic acid MIDA ester including fluorescence subtraction and binning was necessary before individual peaks could be readily distinguished in the spectrum. The SERS spectrum of methylboronic acid MIDA

ester was easily obtained with relatively few scans and was used without any modification.

The success in quenching the fluorescence in methyboronic acid MIDA ester to reveal a SERS spectrum that corroborated previously taken data encouraged us to continue obtaining original data using the newly developed SERS technique. Naphthylboronic acid MIDA ester was thus investigated. The experimental procedure used to obtain SERS data for methylboronic acid MIDA ester was again employed in these studies.

Methanol was first used as the solvent when applying naphthylboronic acid MIDA ester to SERS substrates using the drop method. The resulting SERS spectrum showed no significant peaks. Acetone, benzene, and TMF provided similar results, even when the concentration of naphthylboronic acid MIDA ester in the solvent was varied significantly. Anhydrous diethyl ether was then used as the solvent, and a SERS spectrum was easily obtained. Figure 4.X shows the SERS spectrum obtained for naphthylboronic acid MIDA ester.

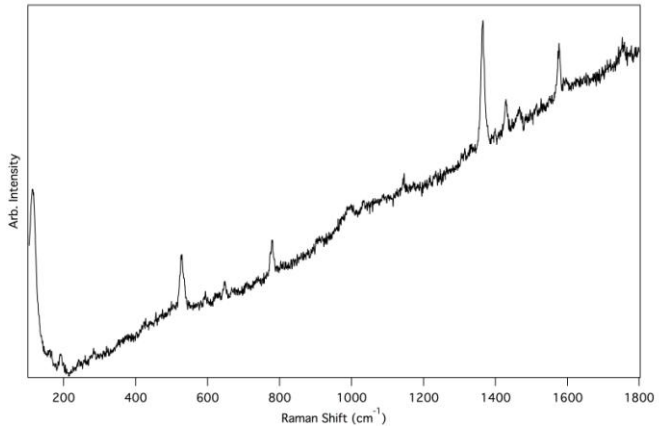

Figure 4.X shows the SERS spectrum obtained by drop coating naphthylboronic acid MIDA ester dissolved in ether.

Fluorescence has been quenched to some extent to reveal peaks, suggesting that the SERS effect is working. The SERS spectrum of naphthylboronic acid MIDA ester was

compared to the modified Raman spectrum and to theory. The results are shown in figure 4.X.

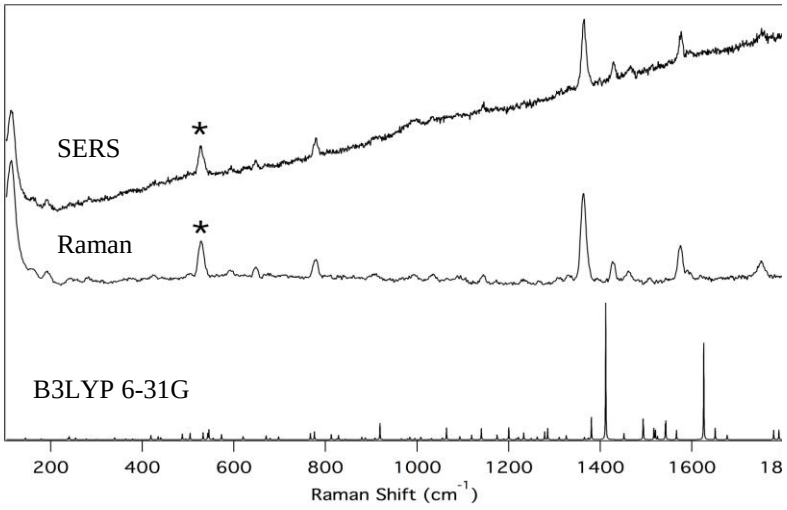

Figure 4.X shows the SERS and Raman spectra of naphthylboronic acid MIDA ester as compared theory from the B3LYP 6-31G

The SERS and modified Raman spectra of naphthylboronic acid MIDA ester provided similar results suggesting the molecule was physisorbed to the SERS substrate. From theory, the B–N stretching frequency was once again assigned at approximately 545 cm^{-1} as indicated in the spectra by a star. Once again, obtaining a SERS spectrum of naphthylboronic acid MIDA ester was trivial once the appropriate solvent was found.

The SERS spectra of methylboronic acid MIDA ester and naphthylboronic acid MIDA ester in vacuum were obtained using the setup described in chapter 3 to obtain SERS spectra of Rhodamine 6G in vacuum. The SERS spectra obtained using this setup were highly distorted. Certain peaks were assigned to vibrational modes but the peak corresponding to the stretching motion of the B–N dative bond was not distinguishable from the background. The spectra are not included for this reason. This difficulty in obtaining good data was attributed to the poor quality and location of the notch filter used to block out the 514.5 nm line of the Argon Ion laser. Purchasing a new notch filter and

better incorporating it in the experimental setup should make obtaining SERS spectra of MIDA esters in vacuum possible.

In conclusion, the SERS spectra of methylboronic acid MIDA ester and naphthylboronic acid MIDA ester were obtained and compared to the modified Raman spectra and theory obtained by Reinemann. In each case, the SERS and Raman spectra looked nearly identical suggesting both MIDA esters were physisorbed to the SERS substrates. The unchanged spectra allowed utilization of Raman theory to assign the stretching frequency of the B–N dative bond to approximately 545 cm^{-1}. The solvent used when depositing each MIDA ester on to the SERS substrates had a profound impact on the observed SERS spectrum. Inappropriate solvents yielded SERS spectra that looked identical to the spectrum of the SERS substrate alone shown in figure 3.5a. SERS spectra obtained using appropriate solvents showed highly resolved peaks. A continuum was present in the background of each obtained SERS spectra, but did not distort the observed peaks. The success of the SERS substrates in quenching much of the fluorescence makes the development of this technique widely applicable.

4.3 References

(1) Pohlki, F.; Doye, S.; *Chemical Society Reviews* **2003**, 32, 104-114.